11 July 1989

FROM: AFIT/CI

SUBJECT: Review of Thesis/Dissertation for Public Release

TO: PA

1. Request you review the attached for public release prior to being sent to DTIC.

2. Reply by indorsement to CI NLT _____.

ERNEST A. HAYGOOD, 1st Lt, USAF
Executive Officer
Civilian Institution Programs

1 Atch
THESIS 89-068
FOGARTY

1st Ind, AFIT/PA

TO: CI

Approved/~~Disapproved~~ for public release.

8 FEB 1990

Log Number: 89-10-109

HARRIET D. MOULTRIE, Capt, USAF
Director, Office of Public Affairs

SECURITY CLASSIFICATION OF THIS PAGE

REPORT DOCUMENTATION PAGE

Form Approved OMB No. 0704-0188

1a. REPORT SECURITY CLASSIFICATION UNCLASSIFIED	1b. RESTRICTIVE MARKINGS NONE
2a. SECURITY CLASSIFICATION AUTHORITY	3. DISTRIBUTION/AVAILABILITY OF REPORT APPROVED FOR PUBLIC RELEASE; DISTRIBUTION UNLIMITED.
2b. DECLASSIFICATION/DOWNGRADING SCHEDULE	
4. PERFORMING ORGANIZATION REPORT NUMBER(S)	5. MONITORING ORGANIZATION REPORT NUMBER(S) AFIT/CI/CIA-89-068
6a. NAME OF PERFORMING ORGANIZATION AFIT STUDENT AT COLORADO STATE UNIVERSITY 6b. OFFICE SYMBOL (If applicable)	7a. NAME OF MONITORING ORGANIZATION AFIT/CIA
6c. ADDRESS (City, State, and ZIP Code)	7b. ADDRESS (City, State, and ZIP Code) Wright-Patterson AFB OH 45433-6583
8a. NAME OF FUNDING/SPONSORING ORGANIZATION 8b. OFFICE SYMBOL (If applicable)	9. PROCUREMENT INSTRUMENT IDENTIFICATION NUMBER
8c. ADDRESS (City, State, and ZIP Code)	10. SOURCE OF FUNDING NUMBERS PROGRAM ELEMENT NO. / PROJECT NO. / TASK NO. / WORK UNIT ACCESSION NO.

11. TITLE (Include Security Classification) (UNCLASSIFIED)
The Invertibility Principle for a Simple Hurricane Model

12. PERSONAL AUTHOR(S)
Robert M. Fogarty

13a. TYPE OF REPORT	13b. TIME COVERED	14. DATE OF REPORT (Year, Month, Day)	15. PAGE COUNT
THESIS/DISSERTATION	FROM _____ TO _____	1989	64

16. SUPPLEMENTARY NOTATION
APPROVED FOR PUBLIC RELEASE IAW AFR 190-1
ERNEST A. HAYGOOD, 1st Lt, USAF
Executive Officer, Civilian Institution Programs

17. COSATI CODES			18. SUBJECT TERMS (Continue on reverse if necessary and identify by block number)
FIELD	GROUP	SUB-GROUP	

19. ABSTRACT (Continue on reverse if necessary and identify by block number)

20. DISTRIBUTION/AVAILABILITY OF ABSTRACT ☒ UNCLASSIFIED/UNLIMITED ☐ SAME AS RPT. ☐ DTIC USERS	21. ABSTRACT SECURITY CLASSIFICATION UNCLASSIFIED
22a. NAME OF RESPONSIBLE INDIVIDUAL ERNEST A. HAYGOOD, 1st Lt, USAF	22b. TELEPHONE (Include Area Code) (513) 255-2259 22c. OFFICE SYMBOL AFIT/CI

DD Form 1473, JUN 86 *Previous editions are obsolete.* SECURITY CLASSIFICATION OF THIS PAGE

AFIT/CI "OVERPRINT"

COLORADO STATE UNIVERSITY

May 30, 1989

WE HEREBY RECOMMEND THAT THE THESIS ENTITLED THE INVERTIBILITY PRINCIPLE FOR A SIMPLE HURRICANE MODEL PREPARED UNDER OUR SUPERVISION BY ROBERT M. FOGARTY BE ACCEPTED AS FULFILLING IN PART REQUIREMENTS FOR THE DEGREE OF MASTER OF SCIENCE.

Committee on Graduate Work

Richard H. Johnson
Committee Member

Gerald D. Taylor
Committee Member

Wayne H. Schubert
Adviser

Department Head

THE INVERTIBILITY PRINCIPLE FOR A SIMPLE HURRICANE MODEL

Author: Robert M. Fogarty

Rank and Service Branch: Capt, USAF

Date: 1989

No. of Pages: 64

Degree: Master of Science — Atmospheric Science

Institution: Colorado State University

ABSTRACT OF THESIS

THE INVERTIBILITY PRINCIPLE FOR A SIMPLE HURRICANE MODEL

We present a reinterpretation of Ooyama's classic tropical cyclone model in terms of the more recent theoretical notions of the potential thickness equation, the potential radius coordinate and the invertibility principle. This helps place tropical cyclone theory in a theoretical framework closer to that of midlatitude theory. We first present a shallow water model of axisymmetric, frictionless flow of homogeneous incompressible fluid on an f- plane. Then we introduce the potential thickness, the inverse of potential vorticity, and write the equation for its evolution. We transform the system from physical space to absolute angular momentum or potential radius space. This eliminates the radial component of the wind from the problem and provides better resolution in areas of large vorticity. We derive and solve the invertibility principle using five different methods– solving for a potential function using the shooting method, the fluid depth using the same method, the fluid depth using a nonlinear equation solving "black box", a transformed velocity using a tridiagonal matrix equation solver, and the transformed velocity with the nonlinear equation solver. The first four methods can not be generalized to two layers. A short review of Ooyama's model shows how the wind field is determined from the radial mass flux. Then we generalize the concepts of the shallow water case to a two layer model using the nonlinear equation solver to solve the invertibility for the transformed velocity.

Robert M. Fogarty
Department of Atmospheric Science
Colorado State University
Fort Collins, Colorado 80523
Summer 1989

ACKNOWLEDGEMENTS

Thanks everybody. In case you don't know who you are — Prof. Wayne Schubert for your patience and wisdom, Prof. Gerald Taylor for finding the "black box" and your suggestions, Prof. Richard Johnson for your help with the content, Paul Ciesielski for your computer expertise and the pretty pictures, Jenny Martin for your help with the manuscript and the anxiety you saved me from, Prof. Scott Fulton for the cubic spline, and my parents, Deanna Ramirez, Kevin Havener, Jim Kossin, Walt Miller, and Mike Meyers et al. for helping me maintain my sanity and your encouragement. Most importantly I thank God for answering my prayers.

Funding for this research was provided by the United States Air Force, Air Force Institute of Technology, Civilian Institution Program. Additional funding was provided by National Science Foundation under Grant ATM 8510664 and its continuation ATM 8814541. Additional funding was provided by ONR Grant N00014-87-K-0535.

TABLE OF CONTENTS

LIST OF FIGURES

Chapter 1

INTRODUCTION

When studying atmospheric dynamics it is often useful to begin with the simplest form. By reducing a problem to its least complicated terms we can learn about its most important features. In 1969 Ooyama presented what is apparently the simplest closed set of equations that describe the life cycle of tropical cyclones. His model has the simplest geometry, moist physics, and the minimum vertical resolution. Ooyama's model can even be thought of as the tropical meteorologist's analogue of the mid-latitude meteorologist's Eady model which is the simplest model of baroclinic instability (Haltiner and Williams, 1980).

The vortex is axisymmetric and described on an f-plane (f, the Coriolis parameter, is constant). The vertical structure is a shallow diagnostic boundary layer and two prognostic main layers above. Moisture is carried only in the boundary layer and only deep convective clouds are parameterized. The simplicity of the model makes it attractive for use in trying different formulations of the physical processes involved in the formation of tropical cyclones.

Some recent advances in atmospheric dynamics can be very useful in the study of tropical cyclones. The use of potential vorticity reasoning (Hoskins et al., 1985; Schubert and Alworth, 1987) in combination with absolute angular momentum, or potential radius, coordinates (Shutts and Thorpe, 1978; Schubert and Hack, 1983) has proven advantageous in this endeavor. The goal here is to introduce these ideas in the framework of Ooyama's model. From the theoretical standpoint this work is concerned with the solution of the invertibility principle.

A historical review of the study of potential vorticity is given by Hoskins et al. (1985). Some of the important early work was done by Rossby. He found (Rossby, 1939) that only

the vertical component of vorticity is important for describing the large scale atmospheric flow. In addition, he was able to produce the barotropic model by assuming the absolute vorticity is conserved following the motion of an air parcel. It is important to note that this model describes two-dimensional horizontal motion. Rossby's later work (1940) gave us perhaps the simplest statement of potential vorticity. He showed that if h is the fluid depth then ζ/h = constant following the motion, where ζ is the absolute vorticity. This equation relates the creation of vorticity by stretching/shrinking of vortex tubes and the horizontal advection of absolute vorticity which are the two processes that are generally most important in the vorticity budget. Ertel (1942), working independently, generalized Rossby's result to three-dimensional, nonhydrostatic flow. He showed that following the motion of an air parcel, the potential vorticity, $P = \rho^{-1}\zeta \cdot \nabla\theta$ = constant, where ρ is the density of the fluid and θ is the potential temperature. Thus, we have the concept of potential vorticity which Hoskins et al. describe as "a potential for creating vorticity by changing latitude and by adiabatically changing the separation of isentropic layers."

Because it is conserved, the potential vorticity was quickly recognized as a Lagrangian tracer. An air parcel can be identified once and for all by its potential vorticity. However, this quantity is much more useful than just a tracer. Hoskins et al. credit Kleinschmidt (1950a,b; 1951, 1955, 1957) with the earliest discovery of this. He recognized that the complete flow structure can be acsertained from the potential vorticity by the inversion of a Laplacian type operator. This idea of recovering the wind field from the potential vorticity field is known as the invertibility principle. For example, in the barotropic case once the vorticity is known, the streamfunction can be calculated, and the winds determined. However, it is not as simple as it first appears. There are three necessary conditions to make invertibility possible. The problem must be solved globally, in reference to a basic state, and under some balance condition (geostrophic, gradient, etc.). The necessity of a balance condition is probably the reason potential vorticity has not been used extensively until recently (Schubert et al., 1986).

Before looking at some recent work using potential vorticity reasoning to describe the structure of tropical cyclones it is useful to examine the potential radius coordinate. In

1978 Shutts and Thorpe used the absolute angular momentum as the radial coordinate in a gradient balance vortex model. They described it as analogous to the use of geostrophic momentum coordinates in the semi-geostrophic equations. This formulation allowed dynamical effects associated with departure from gradient balance to be included implicitly in the same way Hoskins and Bretherton (1972) showed ageostrophic motion is included implicitly in the semigeostrophic theory of frontogenesis. Schubert and Hack (1983) transformed the Eliassen (1952) balanced vortex model to potential radius coordinates and used it to study tropical cyclones. This model describes a slow, quasi-balanced, thermally or frictionally driven axisymmetric vortex. If friction is assumed to be confined to a shallow boundary layer then absolute angular momentum is conserved above it. This allows the use of potential radius above the boundary layer. They introduced this coordinate as a dependent variable in Eliassen's equations then switched the roles of actual radius and potential radius making it the independent variable. The result of this transformation is the stretching of regions of positive relative vorticity and the shrinking of regions of negative relative vorticity. This again is compared to Hoskins and Bretherton's results in their frontogenesis study. These studies show that the potential radius is indeed a useful tool.

The question arises is it worthwhile to create a tropical cyclone model which uses potential vorticity as a predictive variable? One study which suggests the answer is yes is Haynes and McIntyre (1987). They present a theorem on potential vorticity in isentropic layers which they state as

(i) *There can be no net transport of Rossby-Ertel potential vorticity (PV) across any isentropic surface.*

(ii) *PV can neither be created nor destroyed, within a layer bounded by two isentropic surfaces.*

This holds whether or not there is diabatic heating, friction, or other forces. An application of this theorem, presented as a thought experiment, leads to some insight into tropical cyclones. Their experiment involves applying a pulse of cooling to an unbounded, stably

stratified, rotating fluid at rest on an f-plane. If we reverse this and instead apply a pulse of heating (Fig. 1.1) we have a system analogous to a tropical cyclone, the heating being the release of latent heat. If we assume the heating occurs on a time scale much faster than any dynamical adjustment process then by the arguments of Haynes and McIntyre the isentropes adjust by curving as shown in Fig. 1.2. The greatest compaction of the isentropes is just below the area of maximum heating and this creates a positive potential vorticity anomaly in that region while the reverse is true above. They show that these anomalies are the result of horizontal transport and are merely a result of redistribution of potential vorticity along the isentropes. Thus, we can see that the release of latent heat leads to the production of cyclonic relative vorticity at low levels and anticyclonic relative vorticity at upper levels. This is essentially the case in a tropical cyclone.

Let us now look at combining the potential radius with the potential vorticity to study tropical cyclones. The usefulness of this technique was demonstrated by Schubert and Alworth (1987). They also analyzed the balanced vortex equations of Eliassen (1952). They used potential radius, as the horizontal coordinate with potential temperature as the vertical coordinate. This combination of coordinates led to a simple flux form of the inverse potential vorticity equation which separated it from the transverse circulation. Solving the invertibility, a second-order partial differential equation, allowed them to recover the wind field from the potential vorticity. The solutions show that latent heat release generates potential vorticity at low levels and destroys it at upper levels. In addition, vertical advection causes deepening of the low level potential vorticity maximum and pinching off of the upper level potential vorticity minimum. Ultimately, this shows that the potential vorticity used with the potential radius coordinate makes modeling tropical cyclones simpler and leads to better physical understanding.

The work discussed to this point has dealt with balanced vortex models similar to tropical cyclones, but not a closed model. Our goal is to move toward a closed model which incorporates these principles. We begin in chapter 2 by presenting the basic concepts of potential vorticity and potential radius in a shallow water vortex. We start with the equations of motion for axisymmetric, frictionless flow in a shallow layer of homogeneous

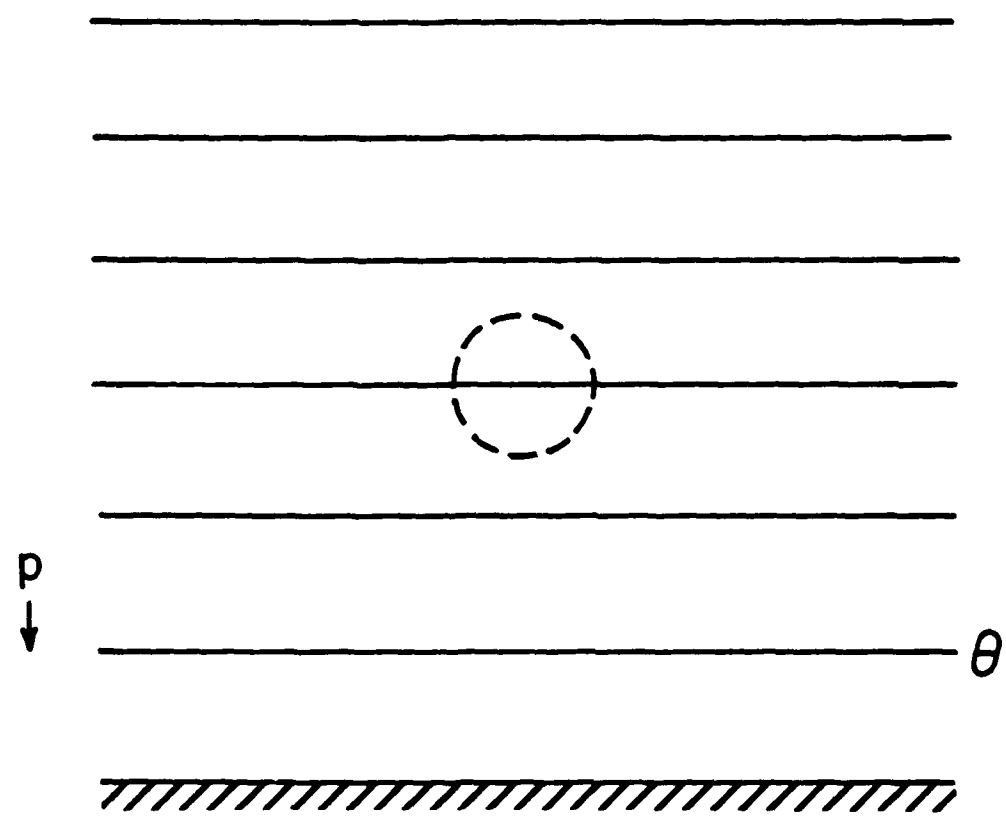

Figure 1.1: Initial state of experiment proposed by Haynes and McIntyre (1987). A pulse of heating (dashed circle) is applied to an unbounded, stably stratified, rotating fluid at rest on an f-plane.

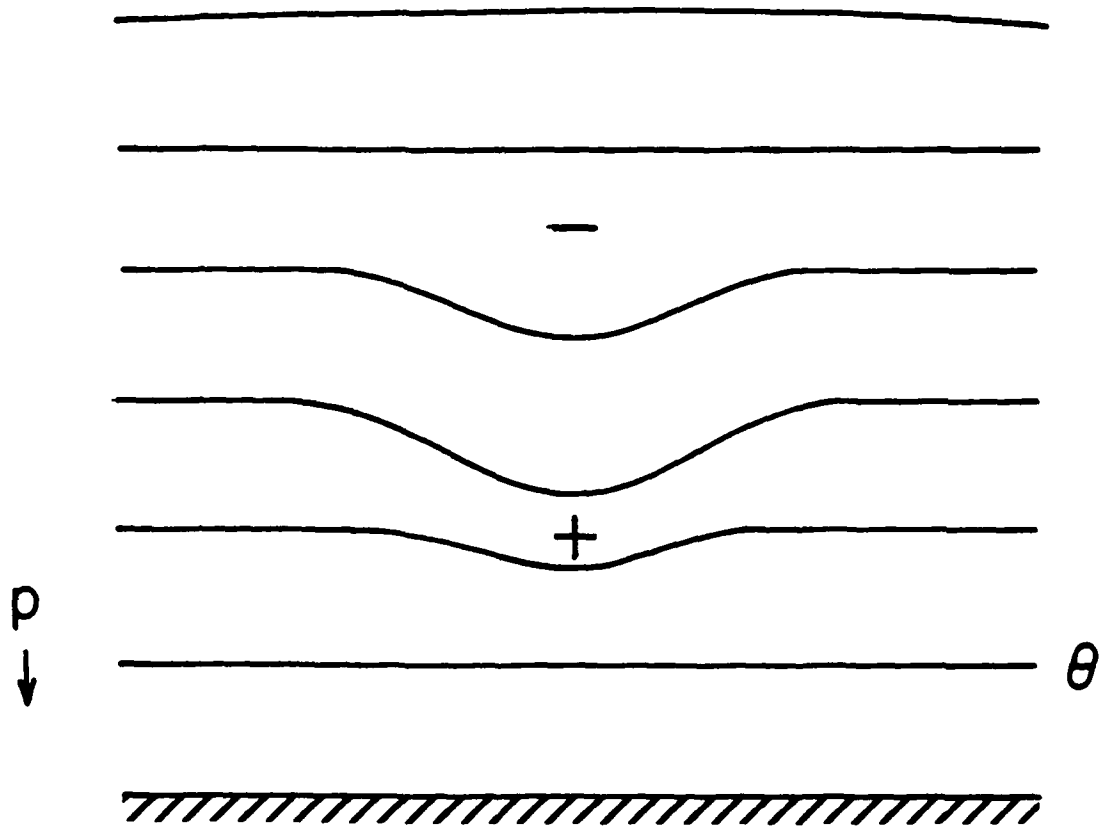

Figure 1.2: Final state of experiment proposed by Haynes and McIntyre (1987). Isentropes have curved in response to heating creating positive potential vorticity anomaly (+) below heating and negative potential vorticity anomaly (−) above.

incompressible fluid on an f-plane. Then we introduce the potential thickness, the inverse of potential vorticity, and write the equation for the evolution of it. This equation, in some sense, describes the release of latent heat. Next we transform the equations to potential radius space. This eliminates the radial wind component from the problem. In chapter 3 we present several different ways to derive and solve numerically the invertibility principle. This problem turned out to be more difficult than expected. We derived several different methods solving for different variables with three different numerical methods–the shooting method, a nonlinear equation solver, and a tridiagonal matrix equation solver. Chapter 4 gives a brief description of Ooyama's model, concentrating on the prediction of the wind field. Then in chapter 5 we generalize these ideas to the full tropical cyclone model. The results of all the methods are presented in chapter 6.

Chapter 2

SHALLOW WATER MODEL

We start by presenting the concepts of potential thickness, potential vorticity, and the invertability principle in a shallow water model.

2.1 Potential thickness equation

We consider axisymmetric, frictionless flow in a shallow layer of homogeneous incompressible fluid on an f-plane. If we assume this flow is in gradient balance, the gradient wind, absolute angular momentum, and mass continuity equations are

$$\left(f + \frac{v}{r}\right)v = \frac{\partial \phi}{\partial r}, \tag{2.1}$$

$$\frac{D}{Dt}\left(rv + \frac{f}{2}r^2\right) = 0, \tag{2.2}$$

$$\frac{Dh}{Dt} + h\frac{\partial (ru)}{r\partial r} = Q, \tag{2.3}$$

where

$$\frac{D}{Dt} = \frac{\partial}{\partial t} + u\frac{\partial}{\partial r} \tag{2.4}$$

is the total derivative, u and v are the radial and tangential components of the wind, $\phi = g(h - \bar{h})$ is the deviation geopotential, h is the fluid depth, and $\bar{h}$ is the undisturbed depth at large radius.

The vorticity equation for this system is derived by expanding the total derivative in (2.2) to obtain

$$\frac{\partial}{\partial t}(rv) + u\frac{\partial}{\partial r}(rv) + \frac{f}{2}u\frac{\partial}{\partial r}(r^2) = 0.$$

Now multiplying the second term on the left hand side by r/r and operating on the entire equation with $\partial/(r\partial r)$ yields

$$\frac{D\zeta}{Dt} + \zeta\frac{\partial (ru)}{r\partial r} = 0, \tag{2.5}$$

where $\zeta = f + \partial(rv)/(r\partial r)$ is the absolute vorticity. Now we use this equation to eliminate the divergence term from (2.3) by multiplying (2.5) by $-h$ and adding ζ times (2.3) to obtain

$$\zeta \frac{Dh}{Dt} - h\frac{D\zeta}{Dt} = \zeta Q.$$

Defining the potential thickness $H = (f/\zeta)h$ we can write

$$\frac{DH}{Dt} = \frac{H}{h}Q. \tag{2.6}$$

Thus, the potential thickness is the depth a column of fluid would obtain if ζ were changed to f while conserving the ratio h/ζ. It is important to note the potential thickness is inversely proportional to the potential vorticity ζ/h.

2.2 Potential radius coordinate

Let us define the potential radius R by $fR^2/2 = rv + fr^2/2$, the right side of which is the absolute angular momentum. According to (2.2), R is conserved following the motion. We now define $T = t$ and transform from (r, t) space to (R, T) space, but note $\partial/\partial t$ implies fixed r while $\partial/\partial T$ implies fixed R. We transform the partial derivatives so that

$$\frac{\partial}{\partial t} = \frac{\partial R}{\partial t}\frac{\partial}{\partial R} + \frac{\partial}{\partial T}, \tag{2.7}$$

$$\frac{\partial}{\partial r} = \frac{\partial R}{\partial r}\frac{\partial}{\partial R}. \tag{2.8}$$

The definitions of R and ζ allow us to wrtite (2.8) as

$$\frac{\partial}{r\partial r} = \frac{\zeta}{f}\frac{\partial}{R\partial R}. \tag{2.9}$$

Notice in regions where ζ is large the spatial derivatives are stretched in R space giving better resolution. Next we transform the total derivative operator (2.4) by substituting in (2.7) and (2.8). Then using the definition of potential radius and noting the conservation of absolute angular momentum, (2.4) becomes

$$\frac{D}{Dt} = \frac{\partial}{\partial T}, \tag{2.10}$$

so that the total derivative looks like a local derivative in (R,T) space. This allows the potential thickness equation (2.6) to be written

$$\frac{\partial H}{\partial T} = \frac{H}{h}Q. \tag{2.11}$$

Thus, transforming to (R,T) space allows us to compute the potential thickness without explicitly determining the radial component of the wind u. This then is the prognostic equation of the model. If the time evolution of the H field can be forecast with (2.11), we can use it to solve an invertibility principle. The derivation and solution of the invertibility is the subject of chapter three.

Chapter 3

THE INVERTIBILITY PRINCIPLE

We now wish to derive an expression, the invertibility principle, which enables us to recover the mass field h form the potential thickness H. The invertibility principle for this problem can be stated in a number of different ways. The challenge is to find one that can be solved efficiently on a personal computer and easily be generalized to two layers. We have explored five different methods of solution for the shallow water case each with its own strengths and weaknesses. In this chapter we will examine these, first revealing the various forms of the invertibility and then discussing the numerical integration methods used with each.

3.1 Method one

Method one involves solving for a new variable Φ. Let us introduce the two new variables Φ and V, defined by

$$\Phi = \phi + \frac{1}{2}v^2, \tag{3.1}$$

$$RV = rv. \tag{3.2}$$

Substituting (3.2) into the definition of absolute vorticity and transforming the result into R space with (2.9) gives

$$\frac{f + \frac{\partial(rv)}{r\partial r}}{f} = \frac{f}{f - \frac{\partial(RV)}{R\partial R}}, \tag{3.3}$$

while from (3.2) and the definition of potential radius we obtain

$$\frac{f + \frac{2v}{r}}{f} = \frac{f}{f - \frac{2V}{R}}, \tag{3.4}$$

so that as $\partial(RV)/(R\partial R)$ approaches f the absolute vorticity becomes infinite, and as $2V/R$ approaches f the absolute circulation per unit area becomes infinite. The definitions (3.1), (3.2), and R along with (3.3) allow us to transform the gradient wind equation (2.1) to

$$\left(\frac{f}{f-\frac{2V}{R}}\right) fV = \frac{\partial \Phi}{\partial R}. \tag{3.5}$$

We now wish to derive the relation between the potential function Φ and the potential thickness H. From (3.1) and the definition of potential radius we get

$$\phi = \Phi - \frac{f^2}{8}\frac{(R^2-r^2)^2}{r^2}. \tag{3.6}$$

Using (2.9) to operate on r and using the definition of potential thickness we get

$$\frac{\partial r}{\partial R} = \frac{R\phi^*}{r\phi}, \tag{3.7}$$

where $\phi^* = gH$. Using the definition of potential radius and (3.2) in (3.5) yields

$$\frac{\partial \Phi}{\partial R} = \frac{f^2 R}{2}\left(\frac{R^2}{r^2}-1\right). \tag{3.8}$$

We solve the system (3.6)–(3.8) for Φ using appropriate boundary conditions.

At the center of the vortex symmetry requires the inner boundary condition to be

$$\frac{d\Phi}{dR} = 0 \quad \text{at} \quad R = 0. \tag{3.9}$$

The lateral boundary condition $\Phi \to \bar{\Phi}$ as $r \to \infty$ must be replaced by an approximate condition at large but finite $r = R = R_b$. To derive this approximate condition suppose that at large r the potential thickness has not been disturbed from its initial value so that $H = \bar{h}$ for large r. We also assume that the lateral boundary is far enough away from any anomalies in the potential thickness that the induced rotational flow at the boundary is weak and approximately geostrophic. Then, the weak flow conditions $|\zeta - f| << \zeta$ and $|\Phi - \bar{\Phi}| << \bar{\Phi}$ allow the definition of potential thickness to be linearized to $(f/\zeta) - 1 + (\phi - \phi^*)/\phi^* = 0$, (3.5) to $fV = \partial\Phi/\partial R$, and (3.6) to $\Phi = \phi$. These relations, along with (3.3), can be combined to yield

$$\frac{d}{RdR}\left(R\frac{d\Phi}{dR}\right) - \mu^2(\Phi - \bar{\Phi}) = 0,$$

where $\mu^2 = f^2/\bar{\Phi}$ and $\bar{\Phi}$ is the undisturbed or basic state value. The solution of this is

$$\Phi = AI_0(\mu R_b) + BK_0(\mu R_b) + \bar{\Phi},$$

where I_0 and K_0 are the modified Bessel functions. We eliminate the I_0 part of the solution, because Φ must be bounded as $R \to \infty$ and use the derivative relation for K_0 to obtain

$$\frac{d\Phi}{dR} + \lambda(\Phi - \bar{\Phi}) = 0 \qquad \text{at large } R, \tag{3.10}$$

where

$$\lambda = \frac{\mu K_1(\mu R_b)}{K_0(\mu R_b)}. \tag{3.11}$$

Using $f = 5.0 \times 10^{-5}$ s^{-1}, $\bar{\Phi} = 5.0 \times 10^3$ m^2 s^{-1}, and $R_b = 1600$ km gives $\lambda = 9.77 \times 10^{-7}$ m^{-1}. Thus, the invertibility principle is defined by (3.6)–(3.11).

3.2 Methods two and three

Methods two and three both solve for h and differ only in the numerical schemes used. We use the definitions of potential radius and the deviation geopotential to write (2.1) as

$$\frac{f^2}{4}\left(\frac{R^4}{r^4} - 1\right) = g\frac{\partial h}{r\partial r}.$$

Now using (2.9) and the definition of potential thickness we get

$$\frac{\partial h}{\partial R} \approx \frac{f^2}{4g}\frac{HR}{h}\left(\frac{R^4}{r^4} - 1\right) \tag{3.12}$$

which relates the slope of the top boundary to the wind field, through the difference between the potential radius and the actual radius, and the thermal field, through the fluid depth. To determine $r(R)$ we use a slightly modified version of (3.7)

$$\frac{\partial r}{\partial R} = \frac{RH}{rh}. \tag{3.13}$$

The boundary conditions here are the same as in method one with h replacing Φ in (3.9) and (3.10).

3.3 Method four

In method four we return to the V variable and derive an expression to solve for it. We start with the definition of potential thickness

$$H = \frac{f}{\zeta} h. \tag{3.14}$$

Using (3.3) in (3.14) and taking $\partial/\partial R$ of the new equation gives

$$-\frac{h}{f}\frac{\partial}{\partial R}\left(\frac{\partial(RV)}{R\partial R}\right) + \frac{f}{\zeta}\frac{\partial h}{\partial R} = \frac{\partial H}{\partial R}. \tag{3.15}$$

Now we substitute (3.12) for $\partial h/\partial R$ to yield

$$-\frac{gh}{f^2}\frac{\partial}{\partial R}\left(\frac{\partial(RV)}{R\partial R}\right) + \left(\frac{f}{\zeta}\right)^2 \frac{f}{4} R\left(\frac{R^4 - r^4}{r^4}\right) = \frac{g}{f}\frac{\partial H}{\partial R}. \tag{3.16}$$

Notice that by factoring $R^4 - r^4$ into $(R^2 + r^2)(R^2 - r^2)$ the second term on the left hand side of this equation becomes

$$\left(\frac{f}{\zeta}\right)^2 \frac{R(R^2 + r^2)}{2r^4}\frac{f}{2}(R^2 - r^2) = \left(\frac{f}{\zeta}\right)^2 \frac{R^2(R^2 + r^2)}{2r^4} V$$

which makes (3.16)

$$-\frac{gh}{f^2}\frac{\partial}{\partial R}\left(\frac{\partial(RV)}{R\partial R}\right) + \left\{\frac{R^2(R^2 + r^2)}{2r^4}\frac{H^2}{h^2}\right\} V = \frac{g}{f}\frac{\partial H}{\partial R} \tag{3.17a}$$

where we've used $H/h = f/\zeta$. Knowing H we solve this equation, with appropriate boundary conditions, for V.

At the center of the vortex symmetry requires that

$$V = 0 \qquad \text{at} \qquad R = 0, \tag{3.17b}$$

and we assume the lateral boundary is far enough from the center that the flow decays to zero. So

$$V = 0 \qquad \text{at} \qquad R = R_b \tag{3.17c}$$

where R_b is some large but finite R.

3.4 Method five

Method five proceeds along as method four does, but continues to eliminate h and r from the invertibility equation. By using the relations (3.3),

$$\frac{r^4}{R^4} = \left(1 - \frac{2V}{fR}\right)^2,$$

and

$$R^2 + r^2 = 2R^2\left(1 - \frac{V}{fR}\right)$$

(3.17a) is written

$$-\frac{\partial}{\partial R}\left(\frac{\partial(RV)}{R\partial R}\right) - \frac{1}{H}\frac{\partial H}{\partial R}\left(f - \frac{\partial(RV)}{R\partial R}\right) + \frac{V\left(f - \frac{V}{R}\right)\left(f - \frac{\partial(RV)}{R\partial R}\right)^3}{gH\left(f - \frac{2V}{R}\right)^2} = 0. \qquad (3.18)$$

which becomes the new statement of the invertibility. The boundary conditions here are the same as in method four.

3.5 Numerical integration

We have devised three different numerical analysis schemes to solve these five systems of equations. Methods one and two are solved using the shooting method with the 4th order Runge-Kutta technique to determine the values of our functions at each grid point and the secant method to solve the lateral boundary condition, methods three and five using a nonlinear equation solver, and method four using a tridiagonal matrix equation solver.

In each case we start by creating a grid in R space and specifying the heating. The grid is set up by letting

$$R_j = j\Delta R, \qquad j = 0, 1, 2, \ldots, J. \qquad (3.19)$$

In addition we include the half points

$$R_{j+\frac{1}{2}} = \left(j + \frac{1}{2}\right)\Delta R, \quad j = 0, 1, 2, \ldots, J \qquad (3.20)$$

where ΔR is the space increment in the horizontal. The heating is determined from (2.11). For the sake of illustrating the nature of the solutions of this equation let $Q/h = S$, which we assume is a known function of R and T. The solution of (2.11) can then be written

$$H(R,T) = H(R,0)\exp\left(\int_0^T S(R,T')dT'\right). \tag{3.21}$$

An interesting consequence of (3.21) is that it is not necessary to compute the solution for all times less than T in order to obtain the solution at time T; only the "total forcing" (the exponent in (3.21)) need be specified. If two solutions happen to have the same distributions of potential thickness, they also have the same distributions of mass and wind since these fields are derived diagnostically from the potential thickness. So let us consider the case in which S has a Gaussian distribution in R and is independent of time. Equation (3.21) then reduces to

$$H(R,T) = H(R,0)e^{\tau(R)}, \tag{3.22}$$

where $\tau(R) = S_0 T\exp(-R^2/R_0^2)$, with the constant S_0 denoting the value of S at $R = 0$. Thus on the grid,

$$H_j = H_0 e^{\tau}, \tag{3.23}$$

where H_0 is specified and,

$$\tau = \hat{Q}T, \tag{3.24}$$

with

$$\hat{Q} = \hat{Q}_0\exp\left(-\frac{R_j^2}{R_0^2}\right) \tag{3.25}$$

where Q_0 is either $+1$ or -1 determining whether there is a mass source or sink and R_0 is the horizontal scale of it. We also determine H at the half points. Fig. 3.1 shows $H(R,T)$ for $H_0 = 500$m, $R_0 = 250$km, $Q_0 = -1$, and $T = 1,2,\ldots,6$ days. Having a solution for H we can solve the invertibility principle and recover the physical fields.

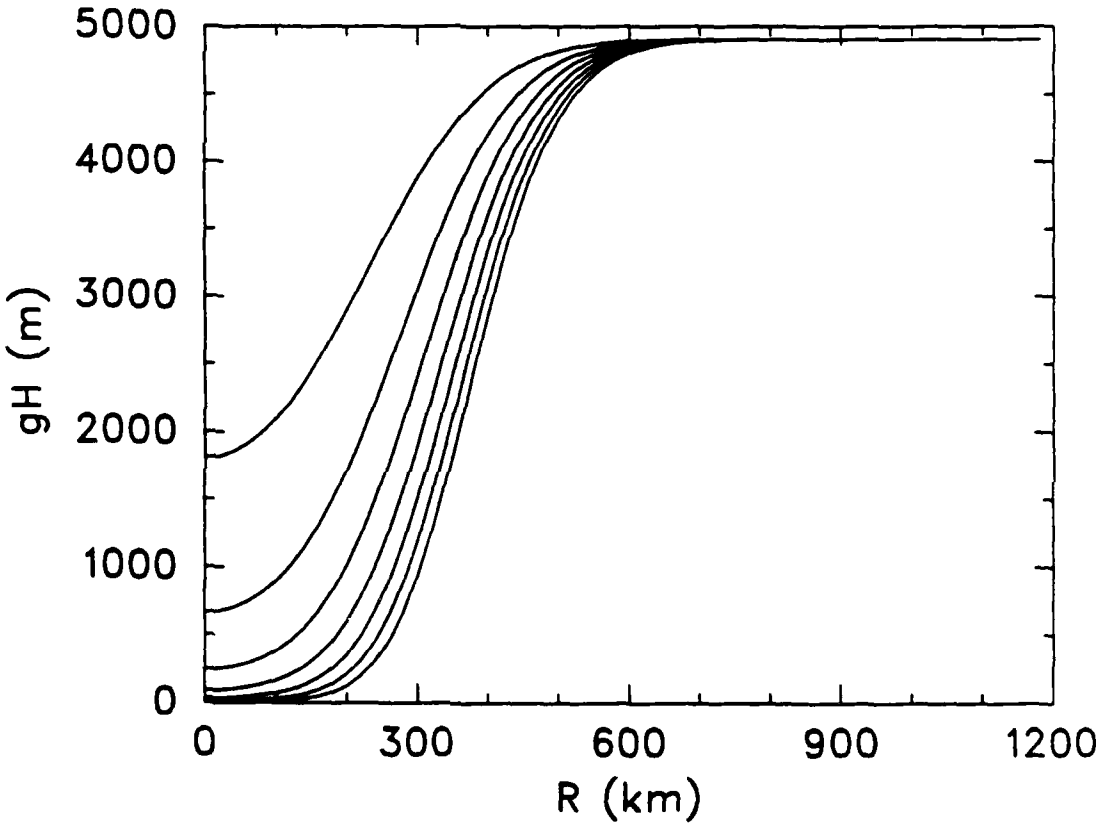

Figure 3.1: The potential thickness H times g as a function of R for $T = 1, 2, \ldots, 7$ days. As fluid is pumped out of the vortex, the potential thickness at the center decreases.

3.5.1 The shooting method

The shooting method (Burden and Faires, 1985) works by integrating (or shooting) from the center to the outer boundary and using the error in the outer boundary condition to make another pass. The values of the functions can be calculated by many techniques. We have chosen to use the 4th order Runge-Kutta method. We use the secant method to reduce the error in the outer boundary condition. Our algorithm proceeds as follows. We make two initial guesses for the variable in question. Then, stepping outward, calculate the value at the lateral boundary and compute an error. The secant method is then used to find a new of value of this variable which is used to start another iteration. Convergence is reached when the error is reduced to an acceptable value. The 4th order Runge-Kutta system is of the form

$$x_{j+1} = x_j + \frac{\Delta R}{6}(k_1 + 2k_2 + 2k_3 + k_4) \tag{3.26}$$

where

$$k_1 = F(R_j, x_j), \tag{3.27}$$

$$k_2 = F\left(R_j + \frac{\Delta R}{2}, x_j + \frac{\Delta R}{2}k_1\right), \tag{3.28}$$

$$k_3 = F\left(R_j + \frac{\Delta R}{2}, x_j + \frac{\Delta R}{2}k_2\right), \tag{3.29}$$

$$k_4 = F(R_{j+1}, x_j + \Delta R k_3). \tag{3.30}$$

and the secant method is

$$x_G^{(NEW)} = \frac{x_G^{(1)}\varepsilon_2 - x_G^{(2)}\varepsilon_1}{\varepsilon_2 - \varepsilon_1} \tag{3.31}$$

where $x_G^{(j)}$ are the guesses for x and ε_j the corresponding errors.

We use a subroutine to calculate the functions F in (3.27)–(3.30). For method one we use the equations

$$\phi_j = \Phi_j - \frac{f^2}{8}\frac{(R_j^2 - r_j^2)^2}{r_j^2}, \tag{3.32}$$

$$\frac{\partial r}{\partial R} = \frac{R_j \phi_j^*}{r_j \phi_j}, \tag{3.33}$$

and

$$\frac{\partial \Phi}{\partial R} = \frac{f^2 R_j}{2}\left(\frac{R_j^2}{r_j^2} - 1\right). \tag{3.34}$$

For method two we use

$$\frac{\partial h}{\partial R} = \frac{f^2}{4g}\frac{H_j R_j}{h_j}\left(\frac{R_j^4}{r_j^4} - 1\right), \tag{3.35}$$

and

$$\frac{\partial r}{\partial R} = \frac{R_j H_j}{r_j h_j}. \tag{3.36}$$

The iteration begins with initial guesses $\Phi = \Phi_G$ or $h = h_G$. We note that as $R \to 0$, $r \to 0$, and (3.33) and (3.36) are not defined. Therefore, we use L'Hospital's rule to get an initial value of r

$$r_0 = \left(\frac{\phi_0^*}{\Phi_G}\right)^{\frac{1}{2}} \tag{3.37}$$

where Φ_G is the guess for Φ. In method two ϕ^* and Φ_G are replaced by H and h_G respectively. The error, ε, in the outer boundary condition is computed from

$$\varepsilon_J = \lambda(\Phi_J - \bar{\bar{\Phi}}) + \frac{3\Phi_J - 4\Phi_{J-1} + \Phi_{J-2}}{2\Delta R} \tag{3.38}$$

where we replace h_j for Φ_j and $\bar{h}$ for $\bar{\bar{\Phi}}$ in method two.

3.5.2 The nonlinear equation solver

Methods three and five use this technique. From a numerical analysis standpoint our problem is solving a system of nonlinear equations of the form

$$\mathbf{F}(\mathbf{x}) = 0,$$

or more specifically in the case of method three $F(h(0)) = 0$, a system of one equation in one unknown, and in method five $F(V_j) = 0$, a system of 79 equations in 79 unknowns. Since this is a fairly common problem we decided to search the literature for existing software to use as a "black box" to solve it. We found a suitable subroutine in Kahaner et. al. (1988). This code requires us to provide an initial guess for the solution and a subroutine to calculate the value of the function. For method three the subroutine that we have devised uses the fourth-order Runge-Kutta method, discussed previously, to solve

for h and r with an initial guess of $h(0) = h_G$. For method five the subroutine solves the finite difference form of (3.18)

$$F_j = \frac{1}{(\Delta R)^2}\left(\frac{R_{j+1}V_{j+1} - R_jV_j}{R_{j+\frac{1}{2}}} - \frac{R_jV_j - R_{j-1}V_{j-1}}{R_{j-\frac{1}{2}}}\right) +$$

$$\left(\frac{1}{H}\frac{\partial H}{\partial R}\right)_j\left(f - \frac{R_{j+1}V_{j+1} - R_{j-1}V_{j-1}}{2R_j\Delta R}\right) - \frac{\left(f - \frac{V_j}{R_j}\right)\left(f - \frac{R_{j+1}V_{j+1} - R_{j-1}V_{j-1}}{2R_j\Delta R}\right)^3}{gH_j\left(f - \frac{2V_j}{R_j}\right)^2}V_j \quad (3.39)$$

with initial guesses of $V_j = 0$.

3.5.3 The tridiagonal matrix solver

When we write (3.17a) in finite difference form we create a system of linear equations in V. If we use matrix notation to solve this system, the coefficient matrix of V is tridiagonal, all the entries are zero except those on the diagonal and on both sides of it. This form is particularly convenient when solving the matrix equation

$$\mathbf{Ax} = \mathbf{b}. \quad (3.40)$$

One method to accomplish this is Crout reduction(Burden and Faires, 1985). If **A** is the coefficient matrix

$$\mathbf{A} = \begin{pmatrix} a_{11} & a_{12} & 0 & \cdots & 0 \\ a_{21} & a_{22} & a_{23} & \ddots & \vdots \\ 0 & \ddots & \ddots & \ddots & 0 \\ \vdots & \ddots & \ddots & \ddots & a_{n-1,n} \\ 0 & \cdots & 0 & a_{n,n-1} & a_{nn} \end{pmatrix},$$

it can be factored into the lower-triangular matrix **L** and the upper-triangular matrix **U** (*LU-decomposition*)

$$\mathbf{L} = \begin{pmatrix} l_{11} & 0 & \cdots & \cdots & 0 \\ l_{21} & l_{22} & \ddots & \ddots & \vdots \\ 0 & \ddots & \ddots & \ddots & \vdots \\ \vdots & \ddots & \ddots & \ddots & 0 \\ 0 & \cdots & 0 & l_{n,n-1} & l_{nn} \end{pmatrix}$$

$$\mathbf{U} = \begin{pmatrix} 1 & u_{12} & 0 & \dots & 0 \\ 0 & 1 & \ddots & \ddots & \vdots \\ \vdots & \ddots & \ddots & \ddots & 0 \\ \vdots & \ddots & \ddots & \ddots & u_{n-1,n} \\ 0 & \dots & \dots & 0 & 1 \end{pmatrix}.$$

Since $\mathbf{A} = \mathbf{LU}$, (3.40) becomes $\mathbf{LUx} = \mathbf{b}$ or

$$\mathbf{Ux} = \mathbf{L}^{-1}\mathbf{b}$$

which we use to solve for $\mathbf{x}$. The LU-decomposition is carried out by noting the multiplications involved in $\mathbf{A} = \mathbf{LU}$

$$a_{11} = l_{11},$$

$$a_{i,i-1} = l_{i,i-1} \qquad \text{for each} \qquad i = 2, 3, \dots, n,$$

$$a_{ii} = l_{i,i-1}u_{i-1,i} + l_{ii} \qquad \text{for each} \qquad i = 2, 3, \dots, n,$$

$$a_{i,i+1} = l_{ii}u_{i,i+1} \qquad \text{for each} \qquad i = 1, 2, \dots, n-1.$$

Once the matrices $\mathbf{L}$ and $\mathbf{U}$ are known we introduce a dummy variable $\mathbf{z}$ and solve

$$\mathbf{Lz} = \mathbf{b}$$

using

$$z_1 = \frac{b_1}{l_{11}}$$

$$z_i = \frac{1}{l_{ii}}(b_i - l_{i,i-1}z_{i-1}) \qquad \text{for each} \qquad i = 2, 3, \dots, n.$$

The final step is to solve

$$\mathbf{Ux} = \mathbf{z}$$

using

$$x_n = z_n$$

$$x_i = z_i - u_{i,i+1}x_{i+1} \qquad \text{for each} \qquad i = n-1, \dots, 1.$$

This form is particularly attractive in our problem, because it updates all of the values at the interior grid points at one time without changing the values at the end points which in our case are always zero.

So we write (3.17a) in finite difference form

$$-\frac{gh_j}{f^2(\Delta R)^2}\left\{\frac{R_{j+1}V_{j+1}-R_jV_j}{R_{j+\frac{1}{2}}}-\frac{R_jV_j-R_{j-1}V_{j-1}}{R_{j-\frac{1}{2}}}\right\}+\left\{\frac{R_j^2(R_j^2+r_j^2)}{2r_j^4}\frac{H_j^2}{h_j^2}\right\}V_j$$

$$=\frac{g}{f}\left(\frac{\partial H}{\partial R}\right)_j \tag{3.41}$$

or the more convenient form

$$-\left(\frac{R_{j-1}}{R_{j-\frac{1}{2}}}\right)V_{j-1}+\left\{\frac{2R_j^2}{R_{j-\frac{1}{2}}R_{j+\frac{1}{2}}}+\frac{R_j^2(R_j^2+r_j^2)}{2r_j^4}\frac{H_j^2}{h_j^2}\frac{f^2(\Delta R)^2}{gh_j}\right\}V_j-\left(\frac{R_{j+1}}{R_{j+\frac{1}{2}}}\right)V_{j+1}$$

$$=\frac{f^2(\Delta R)^2}{gh_j}\frac{g}{f}\left(\frac{\partial H}{\partial R}\right)_j \tag{3.42}$$

Next we determine the coefficient matrix **A** and the right hand side of (3.42). These are passed to a subroutine that performs the LU-decomposition and solves the tridiagonal system. The subroutine passes back a solution for V which we use to update r^2 and h and compute a residual.

Chapter 4

REVIEW OF THE OOYAMA TROPICAL CYCLONE MODEL

4.1 The fluid system and equations of motion

The cyclone-scale motions in Ooyama's model are approximated by a quasi-balanced axisymmetric vortex. It has three vertical levels two of which are prognostic; the other is diagnostic. For simplicity the fluid is assumed to be homogeneous and incompressible. This assumption eliminates any true thermodynamics which is reasonable for adiabatic motions, but can be a problem for diabatic processes. Fortunately, only unstable moist convection involves diabatic motions and this is formulated indirectly in the model.

The system consists of two main layers and a shallow planetary boundary layer. Fig. 4.1 shows a schematic diagram of the fluid system. This allows for the low level cyclone and the upper level anticyclone of the tropical storm. The density of each layer is assumed constant, and the system is stably stratified such that

$$\varepsilon = \frac{\rho_2}{\rho_1} < 1 \quad \text{and} \quad \rho_0 = \rho_1. \tag{4.1}$$

Also important to note are the boundary layer has constant thickness h_0, and the top boundary of the system is a free surface.

For convenience he introduces a reference density ρ such that

$$\rho = \rho_1 = \rho_0 \quad \text{and} \quad \rho_2 = \varepsilon\rho.$$

He also defines the nondimensional static stability

$$\sigma = 1 - \varepsilon. \tag{4.2}$$

Since the fluid is assumed to be incompressible changes in the thickness correspond to adiabatic temperature changes. A layer's thickness can only change by convergence

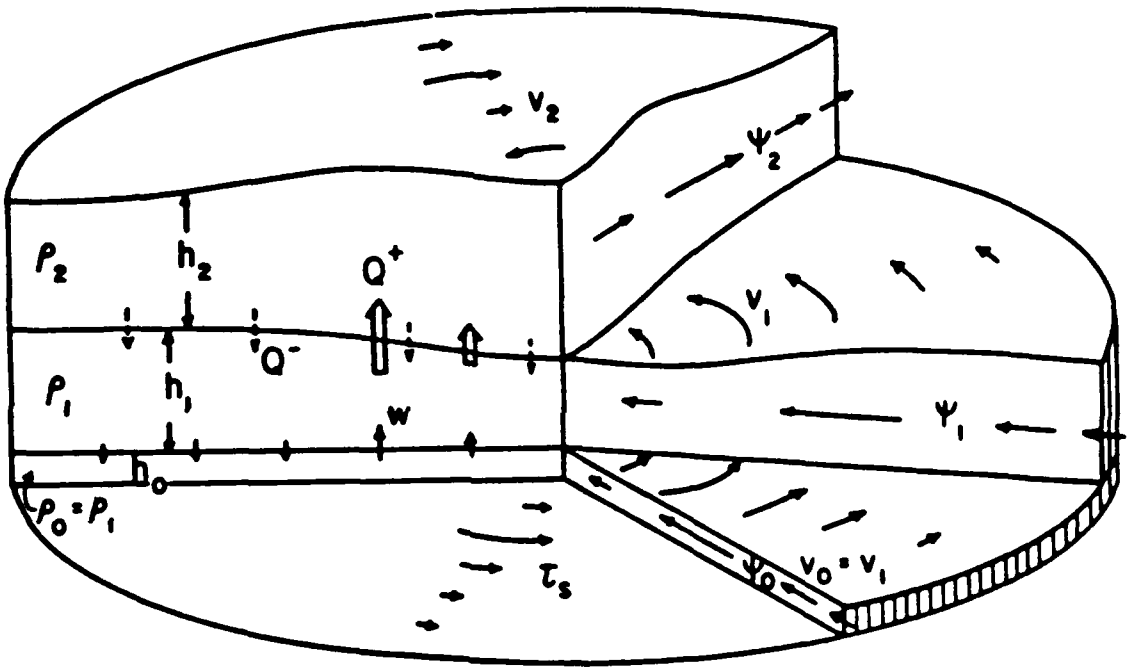

Figure 4.1: Schematic diagram of the fluid system proposed by Ooyama (1969).

and divergence of the fluid caused by the radial wind. The tangential wind can not have any effect on the divergence, because of axisymmetry. Thus the radial mass fluxes, ψ_j for each layer are

$$\psi_0 = -h_0 u_0 r, \tag{4.3}$$

$$\psi_1 = -h_1 u_1 r, \tag{4.4}$$

and

$$\psi_2 = -\varepsilon h_2 u_2 r, \tag{4.5}$$

where u_j is the radial component of the wind defined positive outward. Actually the mass flux is $\rho\psi_j$, but ψ_j is used with little confusion.

Diabatic processes are represented by the change in density of a fluid parcel associated with the vertical motion. Thus, diabatic heating, the movement of air from high density to lower density, is ρQ^+, and diabatic cooling is ρQ^- where Q^+ and Q^- are the diabatic mass fluxes.

Next he writes the mass continuity equations. Since the boundary layer has constant thickness its continuity equation is

$$0 = \frac{\partial \psi_0}{r \partial r} - w \tag{4.6}$$

where w is the vertical velocity at the top of the layer. The equations for the main layers are

$$\frac{\partial h_1}{\partial t} = \frac{\partial \psi_1}{r \partial r} - Q + w \tag{4.7}$$

and

$$\varepsilon \frac{\partial h_2}{\partial t} = \frac{\partial \psi_2}{r \partial r} + Q \tag{4.8}$$

where $Q = Q^+ - Q^-$ is the net diabatic flux.

Using the hydrostatic approximation the pressure in each layer is written

$$p_1 = g\rho(h_0 + h_1 + \varepsilon h_2 - z), \tag{4.9}$$

$$p_2 = \varepsilon g\rho(h_0 + h_1 + h_2 - z), \tag{4.10}$$

and

$$p_0 = p_1 \tag{4.11}$$

where z is the height above the sea level and g is the acceleration due to gravity. Now, if $\bar{h}_j$ and $\bar{p}_j$ denote the undisturbed or average values of h_j and p_j then the deviation geopotential is defined by

$$\phi_j = \frac{p_j - \bar{p}_j}{\rho_j}. \tag{4.12}$$

As previously stated the tangential circulation is represented by a balanced axisymmetric vortex. The radial equation of motion is thus approximated by the gradient wind equation

$$\left(f + \frac{v_j}{r}\right) v_j = \frac{\partial \phi_j}{\partial r} \tag{4.13}$$

where f is assumed constant. Since from (4.12) $\phi_0 = \phi_1$, from (4.13) $v_0 = v_1$.

Ooyama defines the absolute angular momentum for this system as

$$M_j = v_j r + \frac{1}{2} f r^2. \tag{4.14}$$

The angular momentum budgets in each of the main layers is then written

$$\frac{\partial}{\partial t}(h_1 M_1) = \frac{\partial}{r \partial r}(\psi_1 M_1 + \Lambda_1) - Z_{12} + Z_{01} \tag{4.15}$$

and

$$\varepsilon \frac{\partial}{\partial t}(h_2 M_2) = \frac{\partial}{r \partial r}(\psi_2 M_2 + \Lambda_2) + Z_{12} \tag{4.16}$$

where Λ_j are the radial fluxes of angular momentum due to lateral eddy transport, Z_{12} is the vertical flux of angular momentum between the two main layers, and Z_{01} is the vertical flux of angular momentum from the boundary layer to the lower main layer. The model equations are derived from these basic equations.

4.2 The model equations

The equations for Ooyama's model are listed in the box below. A model run consists of predicting ϕ_1 and ϕ_2 with (4.17) and (4.18). In these equations G_l are the diabatic heating terms which are dependent on Q^+. This in turn depends on η which is a nondimensional

parameter developed from energy considerations and is dependent on representative values in layers 0 and 1 of θ_e, an arbitrary constant Θ, and the saturation value in layer 2 θ_e^*. Once ϕ_l is known h_1 and h_2 are determined with (4.19) and (4.20) after which v_1 and v_2 are predicted with (4.21) and (4.22) where F_l are the friction terms.

$$\frac{\partial \phi_1}{\partial t} = g\frac{\partial}{r\partial r}(\psi_1 + \psi_2) + G_1 \tag{4.17}$$

$$\frac{\partial \phi_2}{\partial t} = g\frac{\partial}{r\partial r}(\psi_1 + \varepsilon^{-1}\psi_2) + G_2 \tag{4.18}$$

where $G_1 = gw$ and $G_2 = g(w + \varepsilon^{-1}\sigma Q)$

$$h_1 = \bar{h}_1 + (\sigma g)^{-1}(\phi_1 - \varepsilon\phi_2) \tag{4.19}$$

$$h_2 = \bar{h}_2 + (\sigma g)^{-1}(-\phi_1 + \phi_2) \tag{4.20}$$

$$\frac{\partial (v_1 r)}{\partial t} = h_1^{-1}(f + \zeta_1)\psi_1 + F_1 \tag{4.21}$$

$$\frac{\partial (v_2 r)}{\partial t} = (\varepsilon h_2)^{-1}(f + \zeta_2)\psi_2 + F_2 \tag{4.22}$$

where $\zeta_j = (\partial(v_j r))/(r\partial r)$

$$F_1 = \frac{1}{h_1}\left\{(Q^- + \mu)(v_2 - v_1)r + \frac{\partial \Lambda_1}{r\partial r}\right\} \tag{4.23}$$

$$F_2 = \frac{1}{\varepsilon h_2}\left\{(Q^+ + \mu)(v_1 - v_2)r + \frac{\partial \Lambda_2}{r\partial r}\right\} \tag{4.24}$$

$$Q^- = 0 \tag{4.25}$$

$$Q^+ = \begin{cases} \eta w, & \text{if } w > 0, \\ 0, & \text{if } w \leq 0. \end{cases} \tag{4.26}$$

$$\eta = 1 + \frac{\chi_0 - \chi_2}{\chi_2 - \chi_1} \tag{4.27}$$

where $\chi_0 = (\theta_e)_0 - \Theta$, $\chi_1 = (\theta_e)_1 - \Theta$, and $\chi_2 = (\theta_e^*)_2 - \Theta$

Chapter 5

INCLUSION OF POTENTIAL VORTICITY IN THE OOYAMA TROPICAL CYCLONE MODEL

The closed tropical cyclone model is developed from the basic concepts of the shallow water model with some major modifications. We use a more general fluid system with three layers. The lowest layer represents the moist, cyclonic boundary layer, and the upper two layers represent the cyclonic and anticyclonic flows above. In addition to the more complicated layer system we include surface and internal frictional forces. Absolute angular momentum is no longer conserved with friction included. However, using the potential radius coordinate remains an advantage. In this chapter we generalize the concepts of the shallow water model and derive and solve the invertibility principle for the two main layers of the tropical cyclone model.

5.1 Potential thickness equations

We use the fluid system proposed by Ooyama consisting of three layers, the lowest two having density ρ, and the uppermost having density $\varepsilon\rho$ where $\varepsilon < 1$ so that the system is statically stable. The layer thicknesses are h_0, h_1, and h_2 where h_0 is a constant, and h_1 and h_2 depend on radius and time. We define the deviation geopotentials

$$\phi_1 = g[(h_1 - \bar{h}_1) + \varepsilon(h_2 - \bar{h}_2)] \tag{5.1}$$

and

$$\phi_2 = g[(h_1 - \bar{h}_1) + (h_2 - \bar{h}_2)] \tag{5.2}$$

and write the gradient wind equations for the upper two layers as

$$\left(f + \frac{v_l}{r}\right) v_l = \frac{\partial \phi_l}{\partial r} \tag{5.3}$$

where l is the layer number. Since we assume the hydrostatic approximation and the lower two layers have the same density, they also have the same radial pressure gradient force. If we further assume that the boundary layer is also in gradient wind balance, we conclude that $v_0 = v_1$. Although there is no difference between the tangential wind components in layers 0 and 1, we shall allow a difference between their radial components.

We now turn our attention to the mass conservation and angular momentum principles, both of which provide prognostic equations for the layers above the boundary layer. An objection sometimes raised against the use of a homogeneous incompressible fluid system for tropical cyclone modeling is that it does not include explicit thermodynamics. This objection can be answered by means of analogy. Suppose we consider constant potential temperature layers instead of constant density layers. Then, the geopotential is replaced by the Montgomery potential and the layer thicknesses are replaced by the pressure differences across the isentropic layers. Except for some non-Boussinesq effects the isentropic layer equations turn out to be identical to the isopycnic layer equations. With this in mind, let us consider the isopycnic layer continuity equations

$$\frac{\partial}{r\partial r}(ru_0h_0) + w = 0, \tag{5.4}$$

$$\frac{\partial h_1}{\partial t} + \frac{\partial}{r\partial r}(ru_1h_1) + Q^+ - Q^- - w = 0, \tag{5.5}$$

$$\varepsilon\frac{\partial h_2}{\partial t} + \frac{\partial}{r\partial r}(\varepsilon ru_2h_2) - Q^+ + Q^- = 0, \tag{5.6}$$

where w is the vertical velocity at the top of the boundary layer, ρQ^+ is a vertical mass flux from layer 1 to layer 2, and ρQ^- is a vertical mass flux from layer 2 to layer 1. In the isentropic layer model the analogue of the net mass flux $\rho(Q^+ - Q^-)$ is $\sigma\dot{\theta}$, where $\sigma = -\partial p/\partial\theta$ is the isentropic pseudo-density. Thus, Q^+ represents movement of air from low to high potential temperature (diabatic heating) while Q^- represents movement in the opposite sense (diabatic cooling).

Let us define the absolute angular momentum m_l and the potential radius R_l as $m_l = fR_l^2/2 = rv_l + fr^2/2$. Then, the absolute angular momentum equations can be

written

$$fR_l\dot{R}_l = \begin{cases} \frac{r}{h_0} c_D \,|v_1|\, v_1, & l = 0 \\ \frac{r}{h_1}(Q^- + \mu)(v_2 - v_1), & l = 1 \\ \frac{r}{\epsilon h_2}(Q^+ + \mu)(v_1 - v_2), & l = 2 \end{cases} \tag{5.7}$$

where c_D is the drag coefficient, μ is the constant coefficient for momentum transfer through shearing stress at the interface, and $\dot{R}_l$ is the total derivative of R_l. We have neglected lateral momentum transport due to turbulent eddy processes.

Assuming Q^+ and Q^- can somehow be parameterized, we regard (5.1)–(5.7) as a closed system in u_0, u_1, u_2, v_1, v_2, w, ϕ_1, ϕ_2, h_1, h_2. Since (5.1)–(5.3) diagnostically relate h_1, h_2, v_1, v_2, the prediction of h_1 and h_2 from (5.5) and (5.6) must be consistent with the prediction of v_1 and v_2 from (5.7). This implies a coupled pair of diagnostic equations for u_1 and u_2 (see Equation (4.1) of Ooyama, 1969). This coupled pair can then replace either (5.5) and (5.6) or (5.7). In the next section we adopt a different approach. We first combine (5.5) and (5.6) with (5.7) to obtain the potential thickness (or inverse potential vorticity) equations. These equations contain u_1 and u_2 as advecting velocities. We then transform the independent variable from actual radius to potential radius, which removes u_1 and u_2 from the problem.

Defining the vertical component of absolute vorticity by

$$\zeta_l = \frac{\partial}{r\partial r}\left(\frac{fR_l^2}{2}\right) = f + \frac{\partial(rv_l)}{r\partial r}, \tag{5.8}$$

we can differentiate (5.7) to obtain

$$\frac{\partial \zeta_l}{\partial t} + \frac{\partial}{r\partial r}\left(ru_l\zeta_l - fR_l\dot{R}_l\right) = 0, \tag{5.9}$$

where $fR_l\dot{R}_l$ has been used as shorthand notation for the right hand sides of (5.7). Defining the potential vorticity as $q_l = \zeta_l/h_l$ we can write (5.9) as

$$\frac{\partial}{\partial t}(h_l q_l) + \frac{\partial}{r\partial r}\left(ru_l h_l q_l - fR_l\dot{R}_l\right) = 0. \tag{5.10}$$

Thus, $ru_l h_l q_l - fR_l\dot{R}_l$ can be interpreted as the flux of potential vorticity. This flux is along the layer so that the interfaces between layers are impermeable to potential vorticity.

Integrating over the area within some large radius at which both ru_l and $R_l\dot{R}_l$ vanish we obtain

$$\frac{\partial}{\partial t}\int q_l h_l r dr = 0. \tag{5.11}$$

In this sense the potential vorticity within the layer is indestructible. These two restrictions on the way in which the potential vorticity can change have been clearly discussed by Haynes and McIntyre (1987) and McIntyre (1987).

We can now combine (5.5) and (5.6) with (5.9) to obtain the potential thickness equations. We do this by multiplying (5.5) and (5.6) by f/ζ_l. Now we subtract (5.9) times $(fh_1)/\zeta_1^2$ from (5.5) and (5.9) times $(\varepsilon f h_2)/\zeta_2^2$ from (5.6) to obtain

$$\frac{\partial H_1}{\partial t} + u_1\frac{\partial H_1}{\partial r} + H_1\frac{f}{\zeta_1}\frac{\partial}{r\partial r}(R_1\dot{R}_1)$$

$$+\frac{H_1}{h_1}(Q^+ - Q^- - w) = 0 \tag{5.12}$$

and

$$\frac{\partial H_2}{\partial t} + u_2\frac{\partial H_2}{\partial r} + H_2\frac{f}{\zeta_2}\frac{\partial}{r\partial r}(R_2\dot{R}_2)$$

$$-\frac{H_2}{\varepsilon h_2}(Q^+ - Q^-) = 0 \tag{5.13}$$

where

$$H_l = \frac{f}{\zeta_l}h_l \tag{5.14}$$

is the potential thickness of layer l. Since H_l is the inverse of the potential vorticity, we can interpret H_l as the depth layer l would acquire if ζ_l were changed to f under conservation of the ratio h_l/ζ_l.

5.2 Potential radius coordinate

With (r,t) as independent variables we regard the $R_l(r,t)$ as dependent variables. We now reverse this situation and regard (R,T) as independent variables and $r_l(R,T)$ as dependent variables. We define $T = t$ but note that $\partial/\partial t$ implies fixed r while $\partial/\partial T$ implies fixed R. We transform the partial derivatives to

$$\frac{\partial}{\partial t} = \frac{\partial R_l}{\partial t}\frac{\partial}{\partial R} + \frac{\partial}{\partial T} \tag{5.15}$$

and

$$\frac{\partial}{\partial r} = \frac{\partial R_l}{\partial r}\frac{\partial}{\partial R} \tag{5.16}$$

the second of which combined with the definitions of potential radius and absolute vorticity is written

$$\frac{\partial}{r\partial r} = \frac{\zeta_l}{f}\frac{\partial}{R\partial R}. \tag{5.17}$$

Using (5.15) and (5.16) we write the total derivative

$$\frac{\partial}{\partial t} + u_l\frac{\partial}{\partial r} = \frac{\partial}{\partial T} + \left(\frac{\partial R_l}{\partial t} + u_l\frac{\partial R_l}{\partial r}\right)\frac{\partial}{\partial R}$$

or

$$\frac{\partial}{\partial t} + u_l\frac{\partial}{\partial r} = \frac{\partial}{\partial T} + \dot{R}_l\frac{\partial}{\partial R}. \tag{5.18}$$

Substituting (5.17) and (5.18) into (5.12) and (5.13) gives

$$\frac{\partial H_1}{\partial T} + \frac{\partial}{R\partial R}(R\dot{R}_1 H_1) + (Q^+ - Q^- - w)\frac{H_1}{h_1} = 0 \tag{5.19}$$

and

$$\frac{\partial H_2}{\partial T} + \frac{\partial}{R\partial R}(R\dot{R}_2 H_2) - (Q^+ - Q^-)\frac{H_2}{\varepsilon h_2} = 0, \tag{5.20}$$

which now serve as the prognostic equations of the model. Note that the radial components u_l no longer appear explicitly.

5.3 Invertibility principle

Again we wish to derive expressions for the relationships between h_l and H_l. Following the procedures of method five for the shallow water model we start with the definition of potential thickness (5.14) and then introduce the new variables V_l defined by

$$RV_l = rv_l. \tag{5.21}$$

Substituting (5.21) into (5.8) and transforming the result into R space with (5.17) gives

$$\frac{f + \frac{\partial(rv_l)}{r\partial r}}{f} = \frac{f}{f - \frac{\partial(RV_l)}{R\partial R}}, \tag{5.22}$$

while from (5.21) and the definition of potential radius we obtain

$$\frac{f + \frac{2v_l}{r}}{f} = \frac{f}{f - \frac{2V_l}{R}}, \tag{5.23}$$

so that as the absolute vorticity becomes infinite $\partial(RV_l)/(R\partial R)$ approaches f, and as the absolute circulation per unit area becomes infinite $2V_l/R$ approaches f .

Now using (5.22) in (5.14) and taking $\partial/\partial R$ of the new equation gives

$$-\frac{\partial}{\partial R}\left(\frac{\partial(RV_1)}{R\partial R}\right)+\frac{f}{h_1}\frac{f}{\zeta_1}\frac{\partial h_1}{\partial R}=\left(f-\frac{\partial(RV_1)}{R\partial R}\right)\frac{1}{H_1}\frac{\partial H_1}{\partial R} \tag{5.24}$$

and

$$-\frac{\partial}{\partial R}\left(\frac{\partial(RV_2)}{R\partial R}\right)+\frac{f}{h_2}\frac{f}{\zeta_2}\frac{\partial h_2}{\partial R}=\left(f-\frac{\partial(RV_2)}{R\partial R}\right)\frac{1}{H_2}\frac{\partial H_2}{\partial R} \tag{5.25}$$

which can be written

$$-\frac{\partial}{\partial R}\left(\frac{\partial(RV_1)}{R\partial R}\right)-\frac{1}{H_1}\frac{\partial H_1}{\partial R}\left(f-\frac{\partial(RV_1)}{R\partial R}\right)+\frac{f}{\sigma g H_1}\left(\frac{f}{\zeta_1}\right)^2\sigma g\frac{\partial h_1}{\partial R}=0 \tag{5.26}$$

and

$$-\frac{\partial}{\partial R}\left(\frac{\partial(RV_2)}{R\partial R}\right)-\frac{1}{H_2}\frac{\partial H_2}{\partial R}\left(f-\frac{\partial(RV_2)}{R\partial R}\right)+\frac{f}{\sigma g H_2}\left(\frac{f}{\zeta_2}\right)^2\sigma g\frac{\partial h_2}{\partial R}=0 \tag{5.27}$$

where $\sigma = 1-\varepsilon$. Now we need to find an expression for $\partial h_l/\partial R$. Equations (5.1), (5.2), and the definition of potential radius are used to write (5.3) as

$$\frac{f^2}{4}\left(\frac{R_l^4}{r_l^4}-1\right)=\frac{\partial\phi_l}{r\partial r}.$$

From these two equations, (5.1), and (5.2) we write

$$\frac{f^2}{4}\left(\frac{R_1^4-\varepsilon R_2^4}{\sigma r^4}-1\right)=g\frac{\partial h_1}{r\partial r}$$

and

$$\frac{f^2}{4}\left(\frac{R_2^4-R_1^4}{r^4}\right)=g\sigma\frac{\partial h_2}{r\partial r}.$$

Now using (5.17) and (5.14) we get

$$\frac{\partial h_1}{\partial R}=\frac{f^2}{4g\sigma}\frac{f}{\zeta_1}R\left(\frac{R^4-\varepsilon[R_2(r_1(R))]^4}{[r_1(R)]^4}-\sigma\right) \tag{5.28}$$

and

$$\frac{\partial h_2}{\partial R}=\frac{f^2}{4g\sigma}\frac{f}{\zeta_2}R\left(\frac{R^4-[R_1(r_2(R))]^4}{[r_2(R)]^4}\right). \tag{5.29}$$

We need to be very careful when determining $R_l(r_l(R))$ in these two equations, because of the coordinate transformation and discretization of the model. To illustrate this examine

(5.28). To calculate h_1 we take some arbitrary R. Then we need to find the coresponding R_2 to subtract from it. Because of the coordinate transformation r space is distorted (Fig. 5.1), and we can't simply use the value of R in layer two. We have to find the value of r_1 coresponding to R and then find R_2 on this r surface. This is depicted graphically in Fig. 5.2. To do this we need to know r_j as a function of R. This will be discussed further in the section on the numerical integration.

So, we substitute (5.28) and (5.29) into (5.26) and (5.27) to get

$$-\frac{\partial}{\partial R}\left(\frac{\partial(RV_1)}{R\partial R}\right)-\frac{1}{H_1}\frac{\partial H_1}{\partial R}\left(f-\frac{\partial(RV_1)}{R\partial R}\right)+$$

$$\frac{\left(f-\frac{\partial(RV_1)}{R\partial R}\right)^3}{\sigma g H_1}\frac{R}{4}\left(\frac{R^4-\varepsilon[R_2(r_1(R))]^4}{[r_1(R)]^4}-\sigma\right)=0 \qquad (5.30a)$$

and

$$-\frac{\partial}{\partial R}\left(\frac{\partial(RV_2)}{R\partial R}\right)-\frac{1}{H_2}\frac{\partial H_2}{\partial R}\left(f-\frac{\partial(RV_2)}{R\partial R}\right)+$$

$$\frac{\left(f-\frac{\partial(RV_2)}{R\partial R}\right)^3}{\sigma g H_2}\frac{R}{4}\left(\frac{R^4-[R_1(r_2(R))]^4}{[r_2(R)]^4}\right)=0 \qquad (5.30b)$$

which along with appropriate boundary conditions are the invertibility for the two layer model.

At the center of the vortex symmetry requires that

$$V_l = 0 \qquad \text{at} \qquad R = 0, \qquad (5.30c)$$

and we assume the lateral boundary is far enough from the center that the flow decays to zero. So

$$V_l = 0 \qquad \text{at} \qquad R = R_b \qquad (5.30d)$$

where R_b is some large but finite R.

A model computational cycle consists of predicting new values of H_1 and H_2 using (5.19) and (5.20) followed by solution of (5.30) to obtain V_l. We then solve (5.21) for v_l.

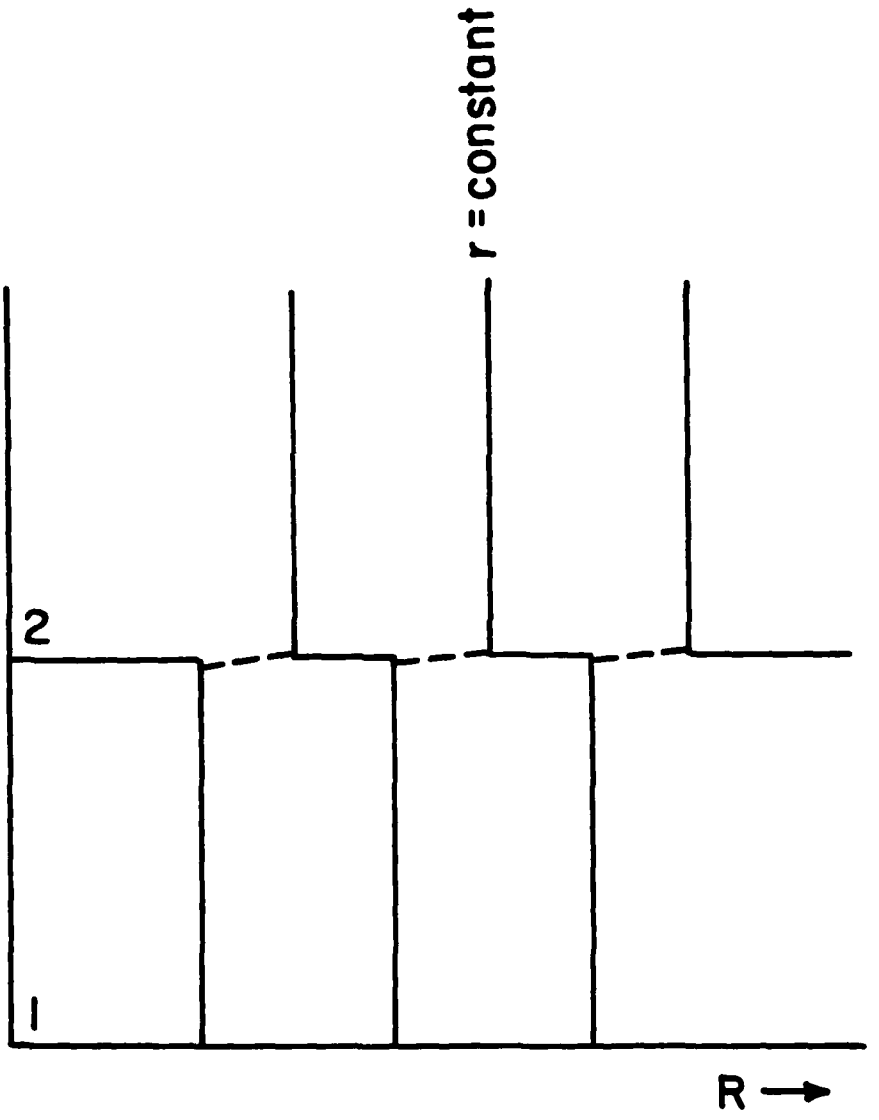

Figure 5.1: The transformed coordinate system. Surfaces of r = constant are distorted in R space.

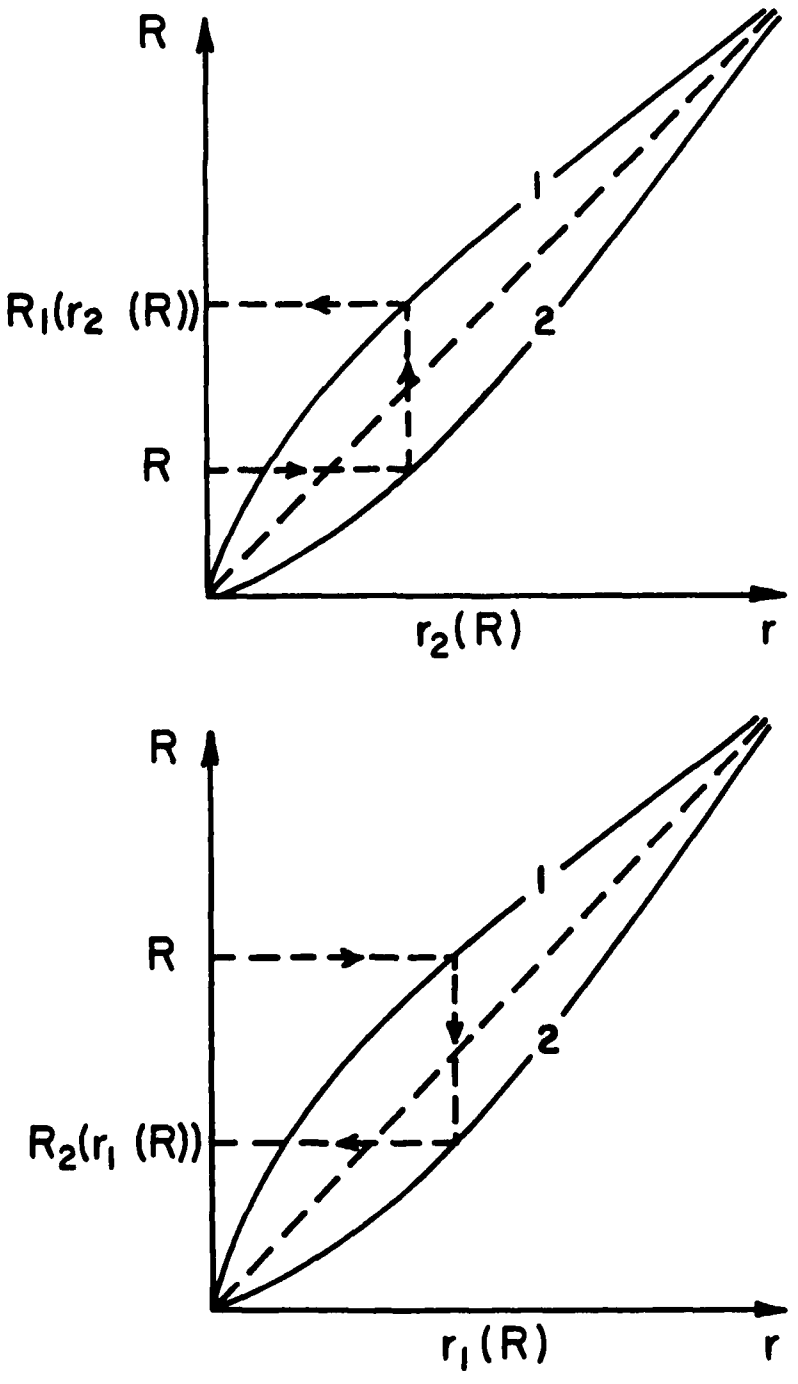

Figure 5.2: Determining $R_l(r_n(R))$. To find $R_1(r_2(R))$ choose an arbitrary R and find the corresponding value on the r_2 curve. Move in the r direction to the r_1 curve and the value corresponding to this as the R axis. The same holds for $R_2(r_1(R))$.

5.4 Numerical integration

We generalize the nonlinear equation solver method developed for the shallow water problem to the tropical cyclone model. Our problem now is solving the system

$$F_l(V_{l,j}) = 0$$

We again use the subroutine from Kahaner et al.(1988) providing guesses $V_{l,j} = 0$. Our system now is 158 equations in 158 unknowns.

The subroutine we provide solves the finite difference forms of (5.30a) and (5.30b). However, to do so we need to know $r_l(R)$ which we find from (5.21)

$$r_{1,j} = R_j\left(1 - \frac{2V_{1,j}}{fR_j}\right)^{\frac{1}{2}} \tag{5.31}$$

$$r_{2,j} = R_j\left(1 - \frac{2V_{2,j}}{fR_j}\right)^{\frac{1}{2}}. \tag{5.32}$$

The finite difference forms of (5.30a) and (5.30b) are

$$F_{1,j} = \frac{1}{(\Delta R)^2}\left(\frac{R_{j+1}V_{1,j+1} - R_jV_{1,j}}{R_{j+\frac{1}{2}}} - \frac{R_jV_{1,j} - R_{j-1}V_{1,j-1}}{R_{j-\frac{1}{2}}}\right) +$$
$$\left(\frac{1}{H_1}\frac{\partial H_1}{\partial R}\right)_j\left(f - \frac{R_{j+1}V_{1,j+1} - R_{j-1}V_{1,j-1}}{2R_j\Delta R}\right) -$$
$$\frac{\left(f - \frac{R_{j+1}V_{1,j+1} - R_{j-1}V_{1,j-1}}{2R_j\Delta R}\right)^3}{\sigma g H_{1,j}}\frac{R_j}{4}\left(\frac{R_j^4 - \varepsilon[R_2(r_1(R_j))]^4}{[r_1(R_j)]^4} - \sigma\right) = 0 \tag{5.33}$$

and

$$F_{2,j} = \frac{1}{(\Delta R)^2}\left(\frac{R_{j+1}V_{2,j+1} - R_jV_{2,j}}{R_{j+\frac{1}{2}}} - \frac{R_jV_{2,j} - R_{j-1}V_{2,j-1}}{R_{j-\frac{1}{2}}}\right) +$$
$$\left(\frac{1}{H_2}\frac{\partial H_2}{\partial R}\right)_j\left(f - \frac{R_{j+1}V_{2,j+1} - R_{j-1}V_{1,j-1}}{2R_j\Delta R}\right) -$$
$$\frac{\left(f - \frac{R_{j+1}V_{2,j+1} - R_{j-1}V_{2,j-1}}{2R_j\Delta R}\right)^3}{\sigma g H_{2,j}}\frac{R_j}{4}\left(\frac{R_j^4 - [R_1(r_2(R_j))]^4}{[r_2(R_j)]^4}\right) = 0 \tag{5.34}$$

The algorithm proceeds as in the single layer case with the grid set up in R space. We then calculate $r_{l,j}$ at the grid points and use a cubic spline routine as another "black box" to create a smooth function. We also use the cubic spline to create $R_2(r_1(R_j))$ and $R_1(r_2(R_j))$. Then when we need values of these we evaluate the splines.

To calculate the heating we assume frictionless flow with $w = 0$ and $Q^- = 0$. This reduces (5.19) to

$$\frac{\partial H_1}{\partial T} + Q^+ \frac{H_1}{h_1} = 0 \tag{5.35}$$

and (5.20) to

$$\frac{\partial H_2}{\partial T} - Q^+ \frac{H_2}{\varepsilon h_2} = 0. \tag{5.36}$$

We now let $S_l = Q^+/h_l$ be some known function of R and T. Now we integrate (5.35) and (5.36) to obtain

$$H_1(R,T) = H_1(R,0) \exp\left(-\int_0^T S_1(R,T')dT'\right) \tag{5.37}$$

and

$$H_2(R,T) = H_2(R,0) \exp\left(\frac{1}{\varepsilon}\int_0^T S_2(R,T')dT'\right). \tag{5.38}$$

Now to illustrate the solutions of (5.37) and (5.38) we let $S = S_1 = S_2/\varepsilon$ be a function with a Gaussian distribution in R and independent of time. Then (5.37) and (5.38) reduce to

$$H_1(R,T) = H_1(R,0)e^{\tau_1(R)} \tag{5.39}$$

and

$$H_2(R,T) = H_2(R,0)e^{\tau_2(R)} \tag{5.40}$$

where $\tau_1(R) = -S_0 T \exp(-R^2/R_0^2)$ and $\tau_2(R) = S_0 T \exp(-R^2/R_0^2)$. This creates a mass sink in layer one and a mass source in layer two.

After H_l is computed at all the grid points, the solution is carried out as in the single layer case. The output variables v_l, h_l, and ζ_l/f are calculated from

$$v_{l,j} = \frac{R_j V_{l,j}}{r_j}, \tag{5.41}$$

$$h_{l,j} = H_{l,j} \frac{f}{f - \frac{\partial(R_j V_{l,j})}{R_j \partial R}}, \tag{5.42}$$

and

$$\frac{\zeta_{l,j}}{f} = \frac{h_{l,j}}{H_{l,j}}. \tag{5.43}$$

Chapter 6

RESULTS

6.1 Shallow water case

Four of the five methods used to solve the shallow water invertibility work very well. They are efficient and able to produce fairly strong vortices. The fifth is efficient, but can produce only a weak vortex. For comparison, each method was run at 168 hours except method four. Method four does not run that far, so it was run at 96 hours. Fig. 6.1 shows the v and ζ/f fields for all five methods. All the methods produce very similar results that resemble a tropical cyclone. The individual results are now presented in more detail.

6.1.1 Methods one and two

Method one works very well. The v and ζ/f fields for this method are shown in Fig. 6.2. It runs to a maximum of 242 hours. At 168 hours it produces a peak wind of 36.66 m/s at $R = 180$ km. The error in the boundary condition is reduced seven orders of magnitude to 10^{-9} in five iterations.

Method two also works very well. It runs to a maximum of 330 hours and at 168 hours (Fig. 6.3) produces a peak wind of 36.41 m/s at $R = 180$ km. The error in the boundary condition here is reduced seven orders of magnitude to 10^{-11} in seven iterations.

However, these methods are hard to generalize to two layers, because of the secant method. The secant method is used to solve a function of a single variable. The two layer model when formulated as in methods one and two is a problem of two equations with two unknowns. Specifically, the errors in the lateral boundary conditions of each layer are dependent on the depths of both layers at the center. Thus, the secant method can not be used to solve this problem.

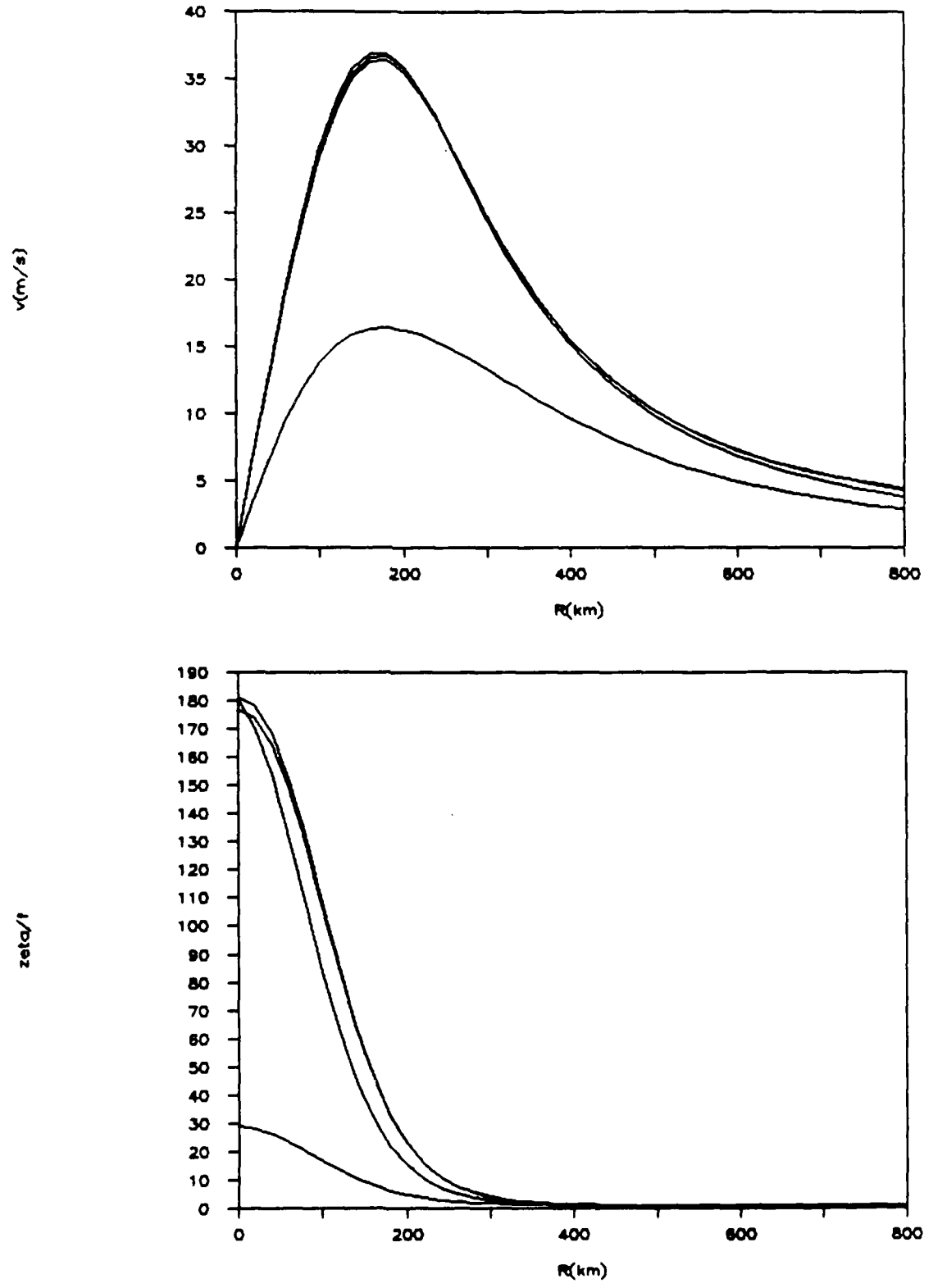

Figure 6.1: Top: The tangential wind (v) as a function of R for all five solution methods and $T = 7$ days (Method four $T = 4$ days.). Bottom: The normalized vorticity (ζ/f) as a function of R. All else the same.

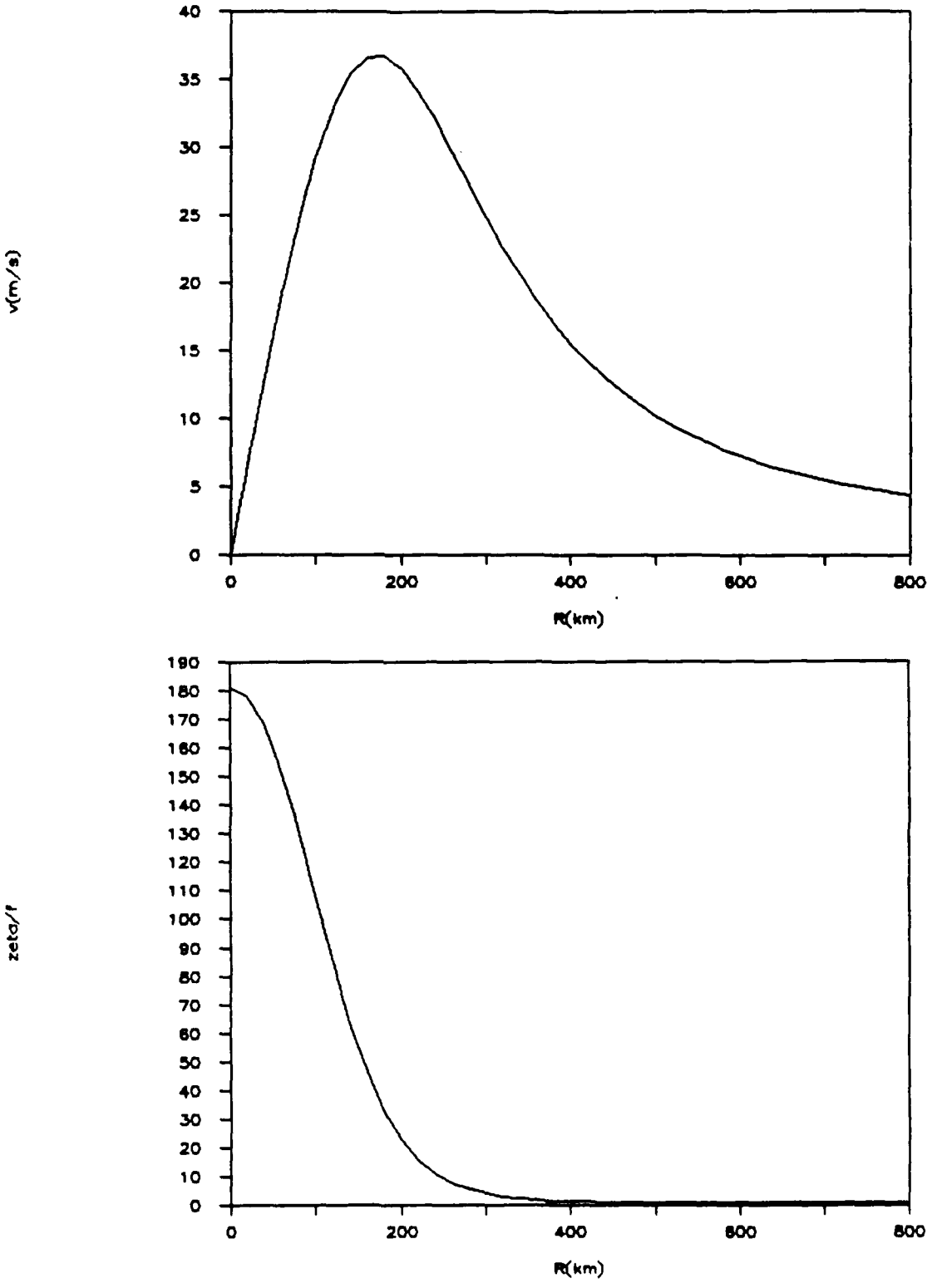

Figure 6.2: Top: The tangential wind (v) as a function of R for method one ($T = 7$ days). Bottom: The normalized vorticity (ζ/f) as a function of R for method one ($T = 7$ days).

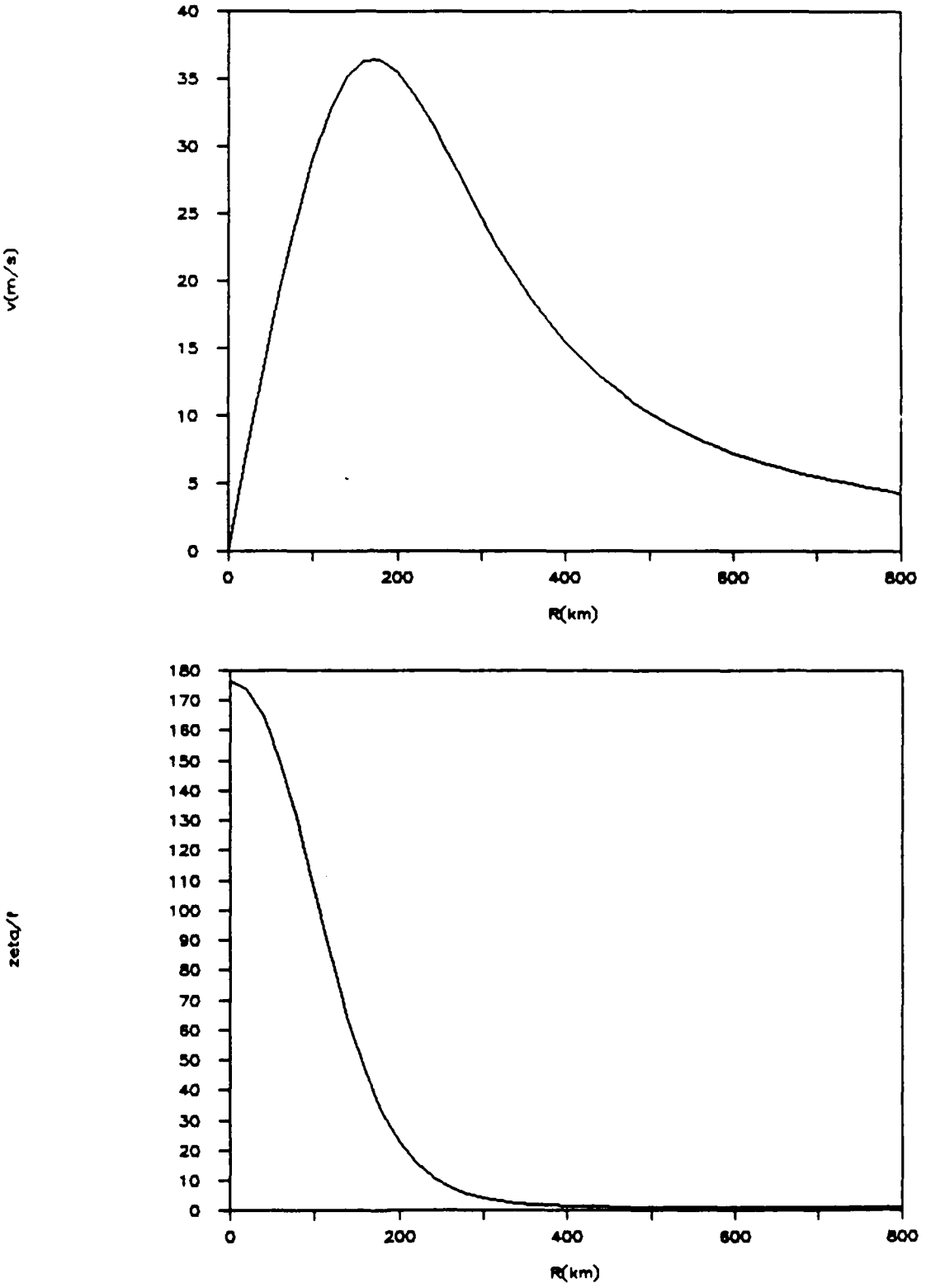

Figure 6.3: Top: The tangential wind (v) as a function of R for method two ($T = 7$ days). Bottom: The normalized vorticity (ζ/f) as a function of R for method two ($T = 7$ days).

6.1.2 Method three

Method three is slightly slower than one and two, but still works very well. It runs to a maximum of 360 hours. At 168 hours (Fig. 6.4) it produces a peak wind of 36.41 m/s at $R = 180$ km. The error in the lateral boundary condition is reduced thirteen orders of magnitude to 10^{-11} in nine iterations. Again this method is hard to generalize. The problem is not well defined in two layers. The error in the outer boundary condition is not uniquely determined by the guesses of $h_l(0)$. The problem is the coordinate transformation. As previously stated when we make the coordinate transformation and discretetize the two layer model we have to interpolate $R_l(r_n(R))$. When we use the nonlinear equation solver the interpolation is done separately and is not constrained in any way. Thus, if we choose different interpolations we would expect the nonlinear equation solver to produce different results. So, we can not uniquely define the problem to be solved.

6.1.3 Method four

Method four does not work well. It runs to a maximum of only 108 hours and to get it that far we have to use previous solutions as initial guesses. At 96 hours (Fig. 6.5) it produces a peak wind of 16.43 m/s at $R = 180$ km. The problem here seems to be in computing the diagonal of the coefficient matrix for (3.42). The tridiagonal solver gets very sensitive as the vorticity gets large and produces infinite vorticity in a fairly short time.

6.1.4 Method five

Method five is the one we've been looking for. It works well, but is somewhat slow. While the other methods all ran in seconds, this one runs in approximately two minutes. However, we were able to generalize it with good results. In the shallow water case at 168 hours (Fig. 6.6) it produces a peak wind of 36.93 m/s at $R = 160$ km.

Since this method is the one we used to solve the two layer case a more complete output set is included. Fig. 6.7 shows the $V(R)$ fields corresponding to the $H(R,T)$ fields in Fig. 3.1. Fig. 6.8 shows the corresponding $v(r)$ fields computed from (3.2). Note that as the r at which the peak $v(r)$ occurs decreases with time, the R at which the peak $V(R)$

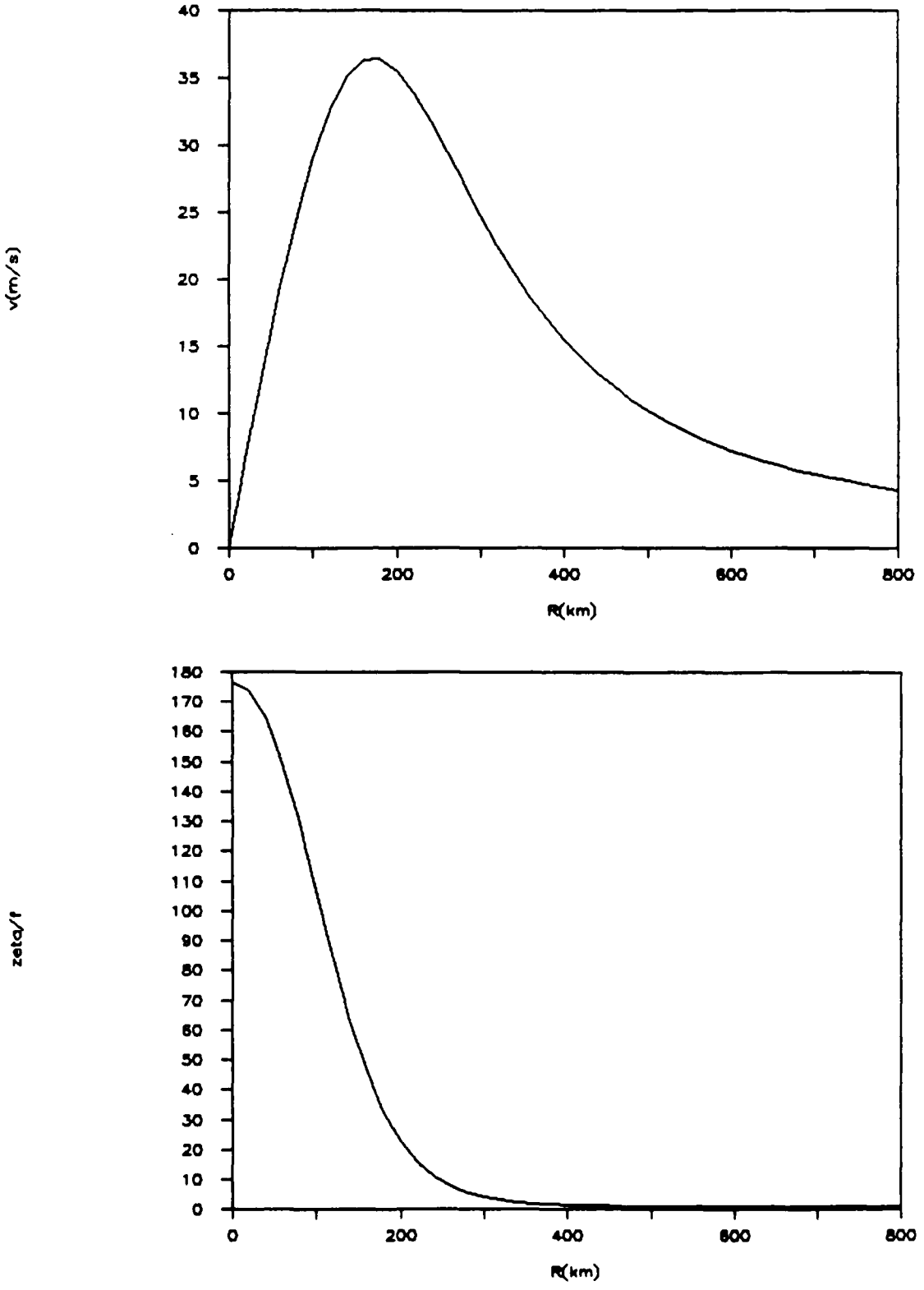

Figure 6.4: Top: The tangential wind (v) as a function of R for method three ($T = 7$ days). Bottom: The normalized vorticity (ζ/f) as a function of R for method three ($T = 7$ days).

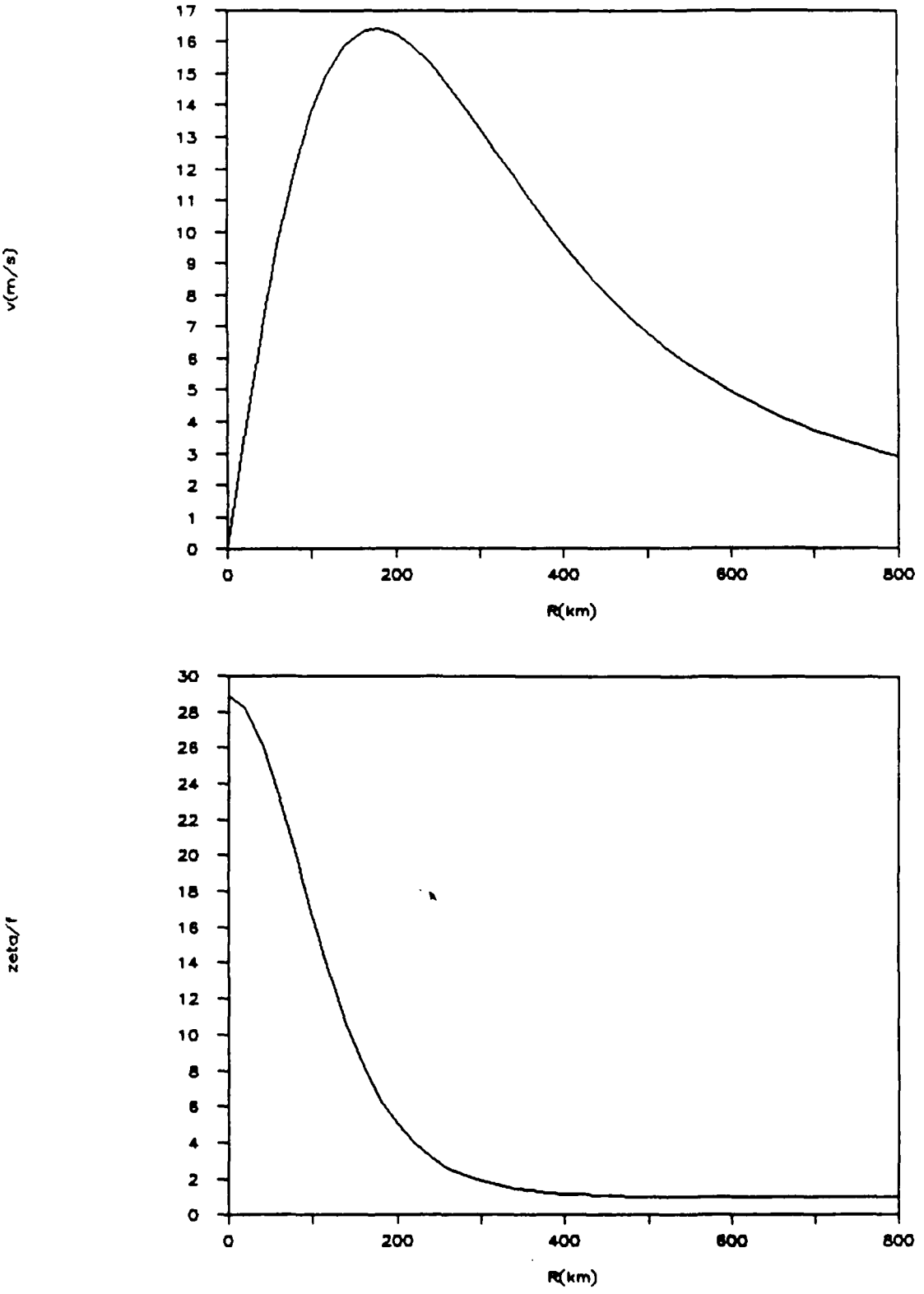

Figure 6.5: Top: The tangential wind (v) as a function of R for method four (T = 4 days). Bottom: The normalized vorticity (ζ/f) as a function of R for method four (T = 4 days).

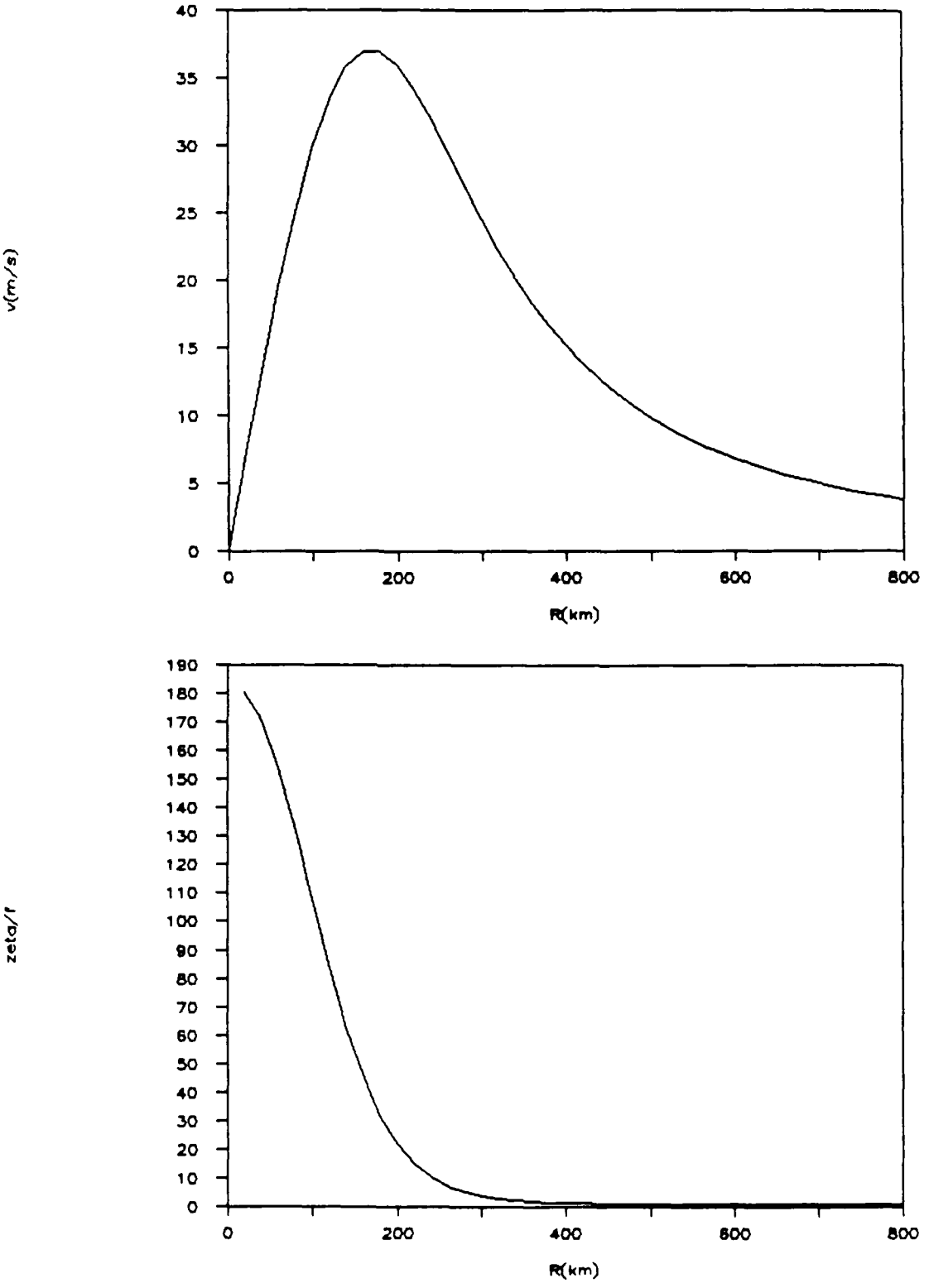

Figure 6.6: Top: The tangential wind (v) as a function of R for method five (T = 7 days). Bottom: The normalized vorticity (ζ/f) as a function of R for method five (T = 7 days).

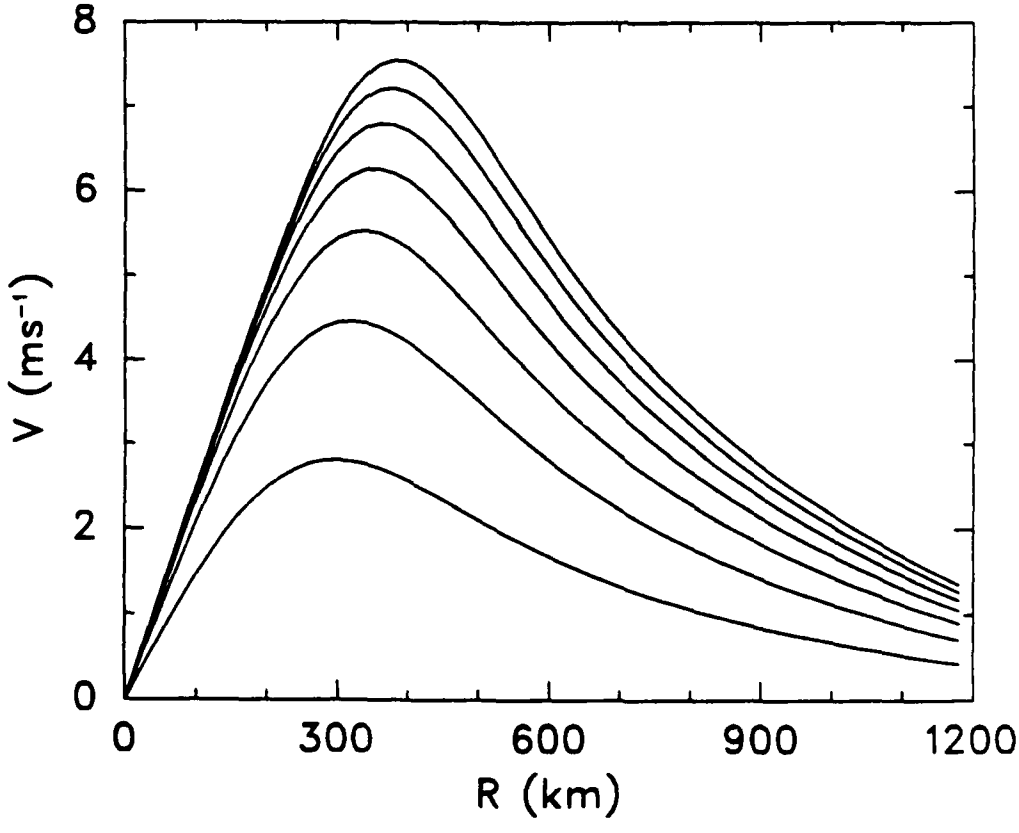

Figure 6.7: V as a function of R for method five corresponding to the $H(R,T)$ fields in Fig. 3.1.

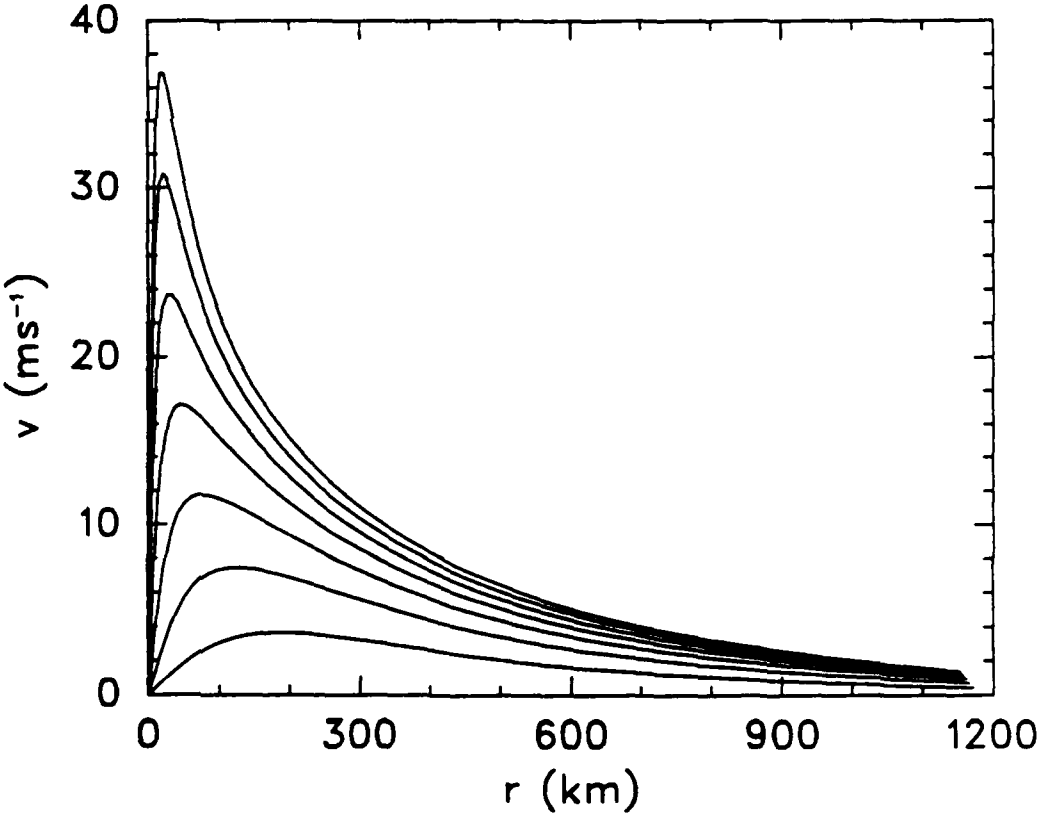

Figure 6.8: The tangential wind (v) as a function of r for method five corresponding to the $H(R,T)$ fields in Fig. 3.1.

occurs increases with time. This is a consequence of (3.3)—stretching in regions of large vorticity.

Another way to view the solutions is shown in Figs. 6.9–6.11. Fig. 6.9 shows the r space distributions of H and Figs. 6.10 and 6.11 show its factors h and f/ζ. We see that as the mass sink forces changes in the potential thickness, the fluid responds by mutually adjusting the mass field, h, and the wind field, ζ/f, to maintain gradient balance. Which is adjusted more, the mass field or the wind field? From Fig. 6.9 H at the center of the vortex is initially fairly low. At the same time h is very high while ζ/f is small. Thus, initially the wind field makes a greater contribution to H. As the system evolves, H gets lower as does h, but ζ/f gets very large. So, with time the contributions from h and ζ/f approach each other. Thus, the mass field adjusts to the wind field.

6.2 The two layer model

The results shown for the two layer model are for the heating given in (5.39) and (5.40) with $H_1(R,0) = 5133.0$ m, $H_2(R,0) = 3523.8$ m, $R_0 = 250$ km, and $\tau_2 = -0.5\tau_1$. The model was run at $S_0T = 1,2,\ldots,7$ and $f = 5.0 \times 10^{-5}\text{s}^{-1}$. Fig. 6.12 shows the $H(R,T)$ field in layer one for the times listed above.

The results show good tropical cyclone structure. The lower layer is as in the single layer case. Fig. 6.13 shows $V(R)$ and again we get the radius of maximum "wind" increasing with time while, as can be seen from Fig. 6.14, the radius of maximum actual wind decreases with time. Figs. 6.15 and 6.16 show $h(r)$ and ζ/f. As noted in the shallow water case they depict the adjustment of the mass field and the wind field. The adjustment here is in the same sense. As the potential vorticity field evolves the contribution from the mass field increases and the contribution from the wind field decreases.

The results from the upper layer show some interesting features. Fig. 6.17 shows $v(r)$. We see that the upper level anticyclone intensifies with time and is pushed outward. This is also evident in Fig. 6.18 which shows $V(R)$. However, in this case the radius of maximum "wind" decreases. The fluid depth and vorticity fields (not pictured) show some of the features we would expect, increasing fluid depth and decreasing vorticity with

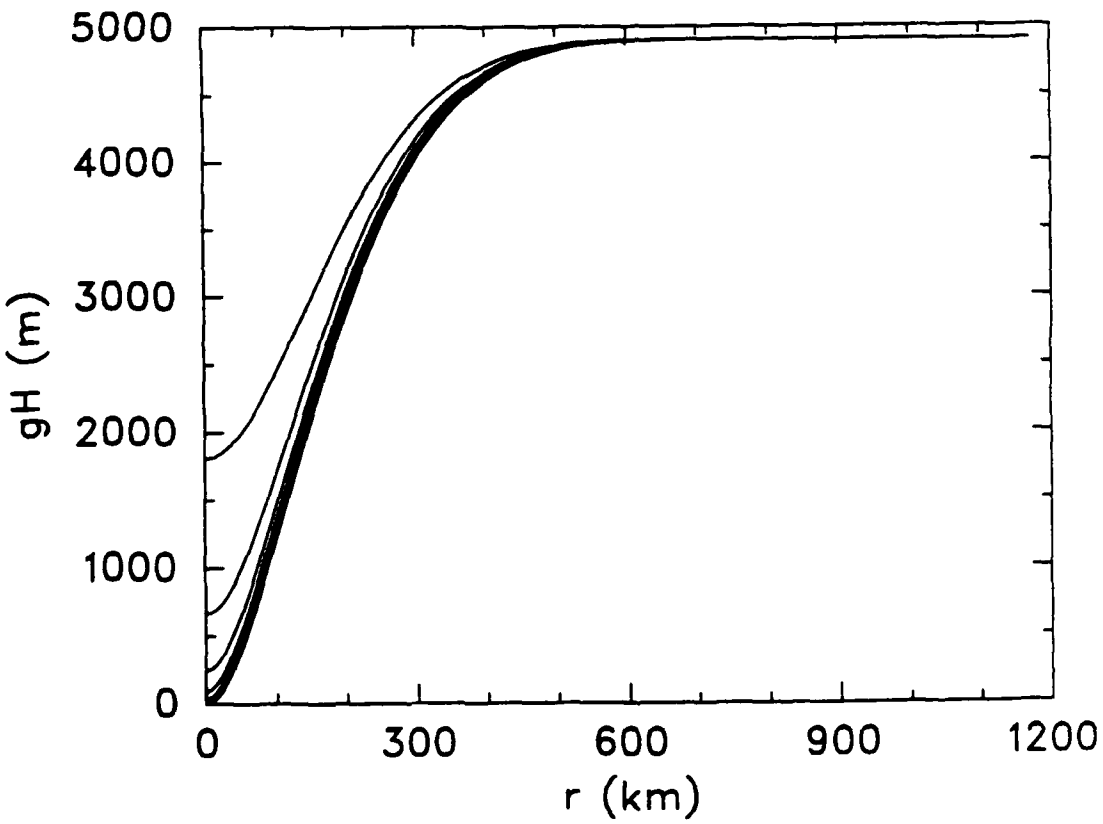

Figure 6.9: The potential thickness (H) times g as a function fo r for method five corresponding to the $H(R,T)$ fields in Fig. 3.1.

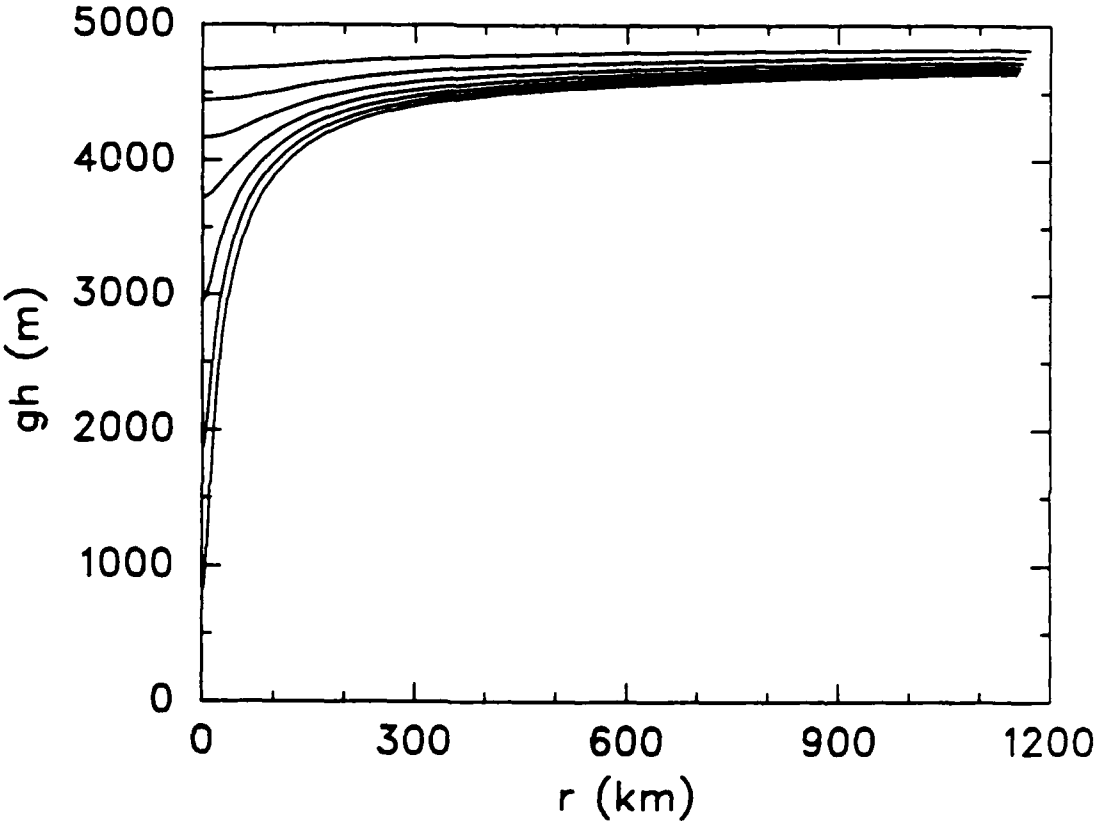

Figure 6.10: The fluid depth (h) times g as a function of r for method five corresponding to the $H(R,T)$ fields in Fig. 3.1.

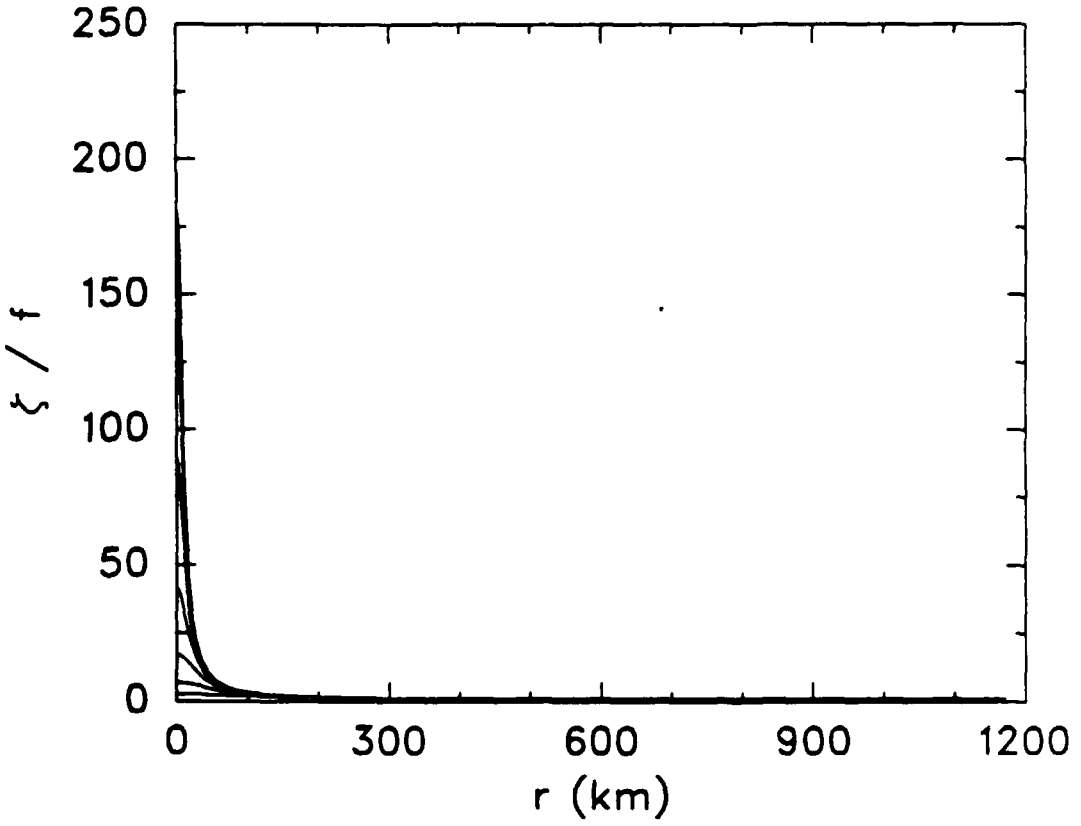

Figure 6.11: The normalized vorticity (ζ/f) as a function of r for method five corresponding to the $H(R,T)$ fields in Fig. 3.1.

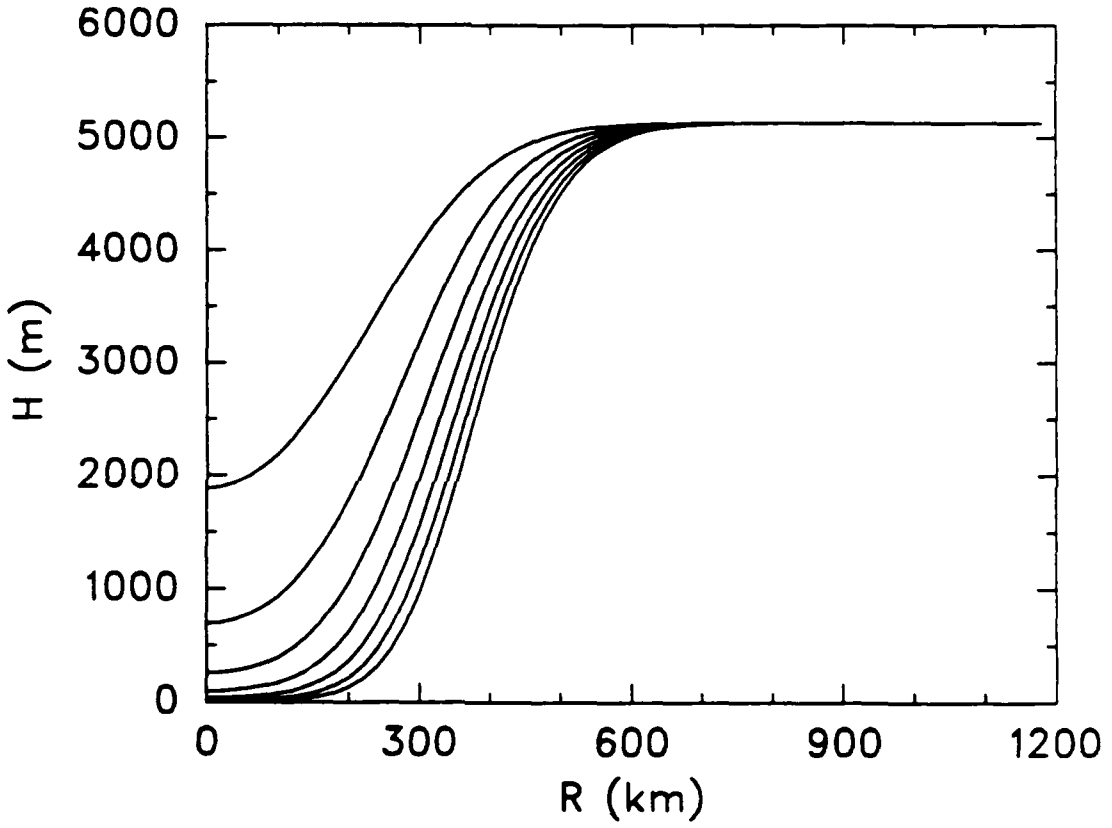

Figure 6.12: The potential thickness (H) in layer one as a function of R and $T = 1, 2, \ldots, 7$ days. As fluid is pumped from layer one to layer two, the potential thickness decreases at the center of the vortex in layer one.

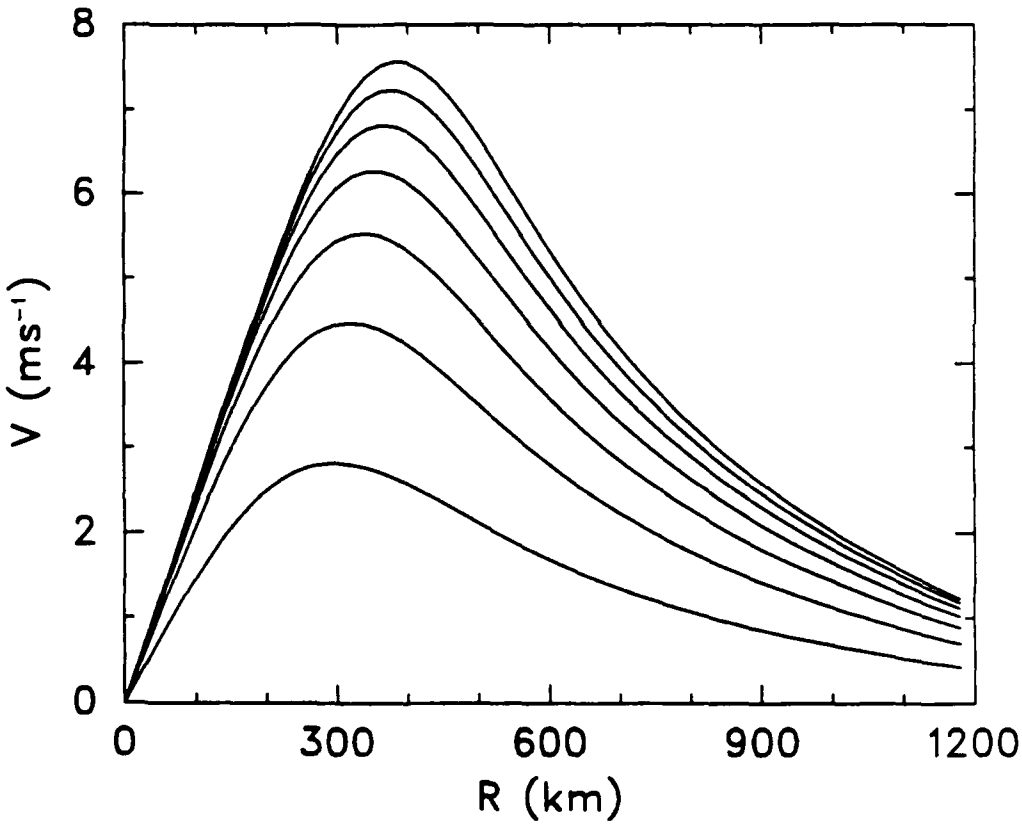

Figure 6.13: V as a function of R for layer one corresponding to the $H(R,T)$ fields in Fig. 6.12.

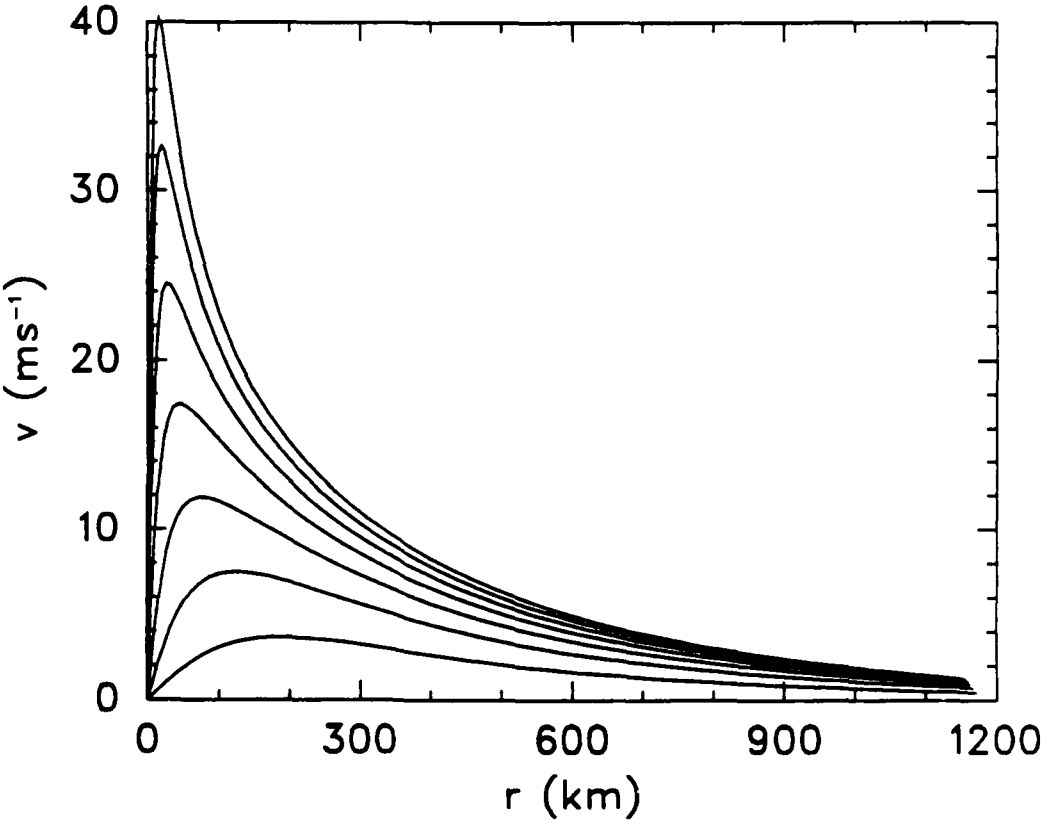

Figure 6.14: The tangential wind (v) as a function of r for layer one corresponding to the $H(R,T)$ fields in Fig. 6.12.

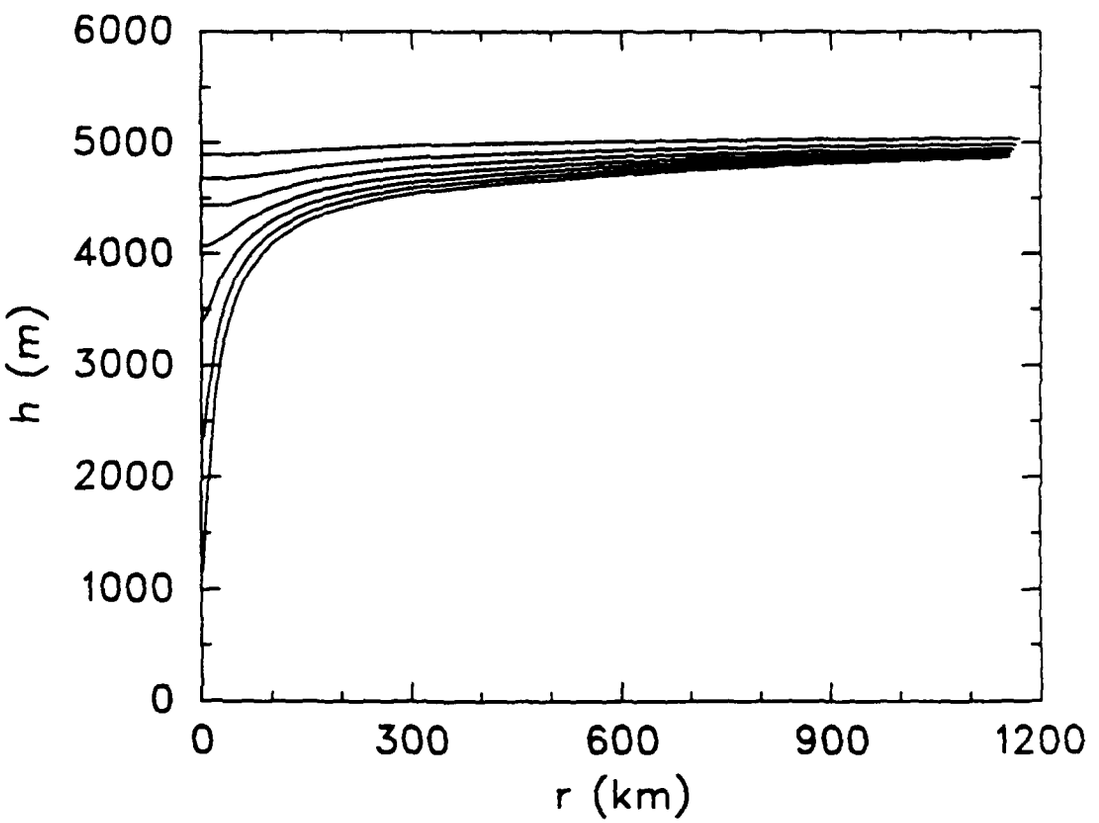

Figure 6.15: The fluid depth (h) as a function of r for layer one corresponding to the $H(R,T)$ fields in Fig. 6.12.

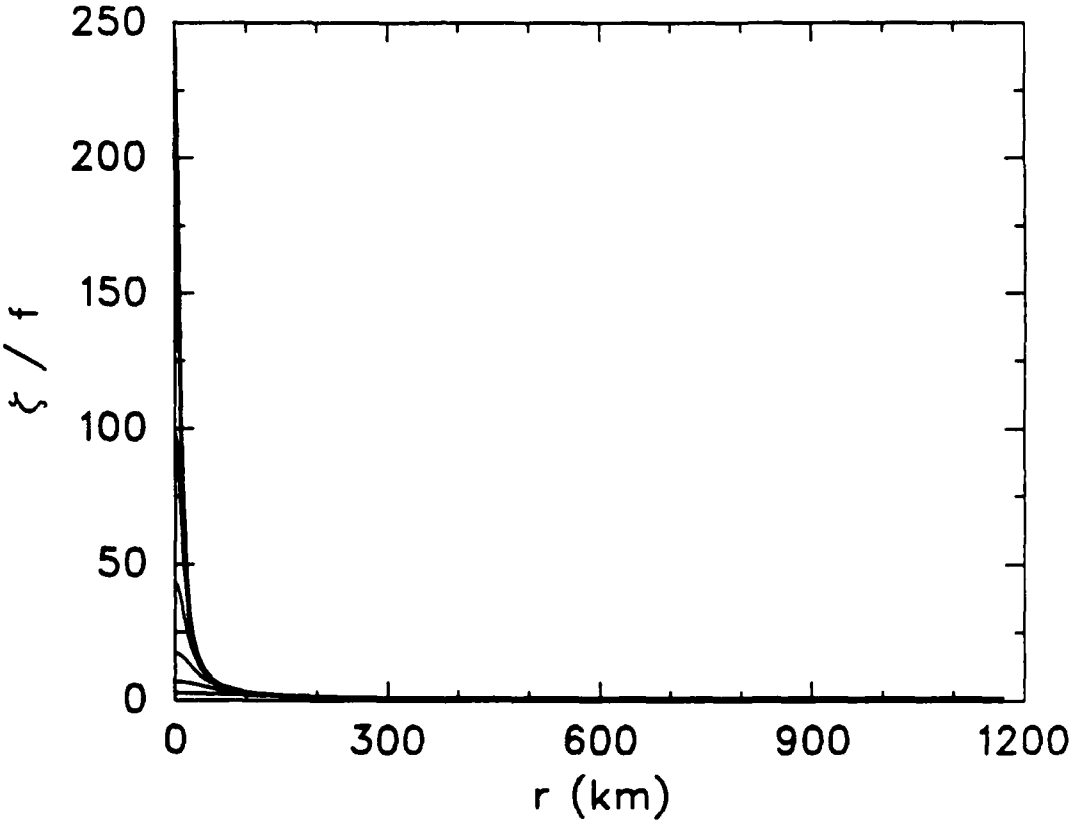

Figure 6.16: The normalized vorticity (ζ/f) as a function of r for layer one corresponding to the $H(R,T)$ fields in Fig. 6.12.

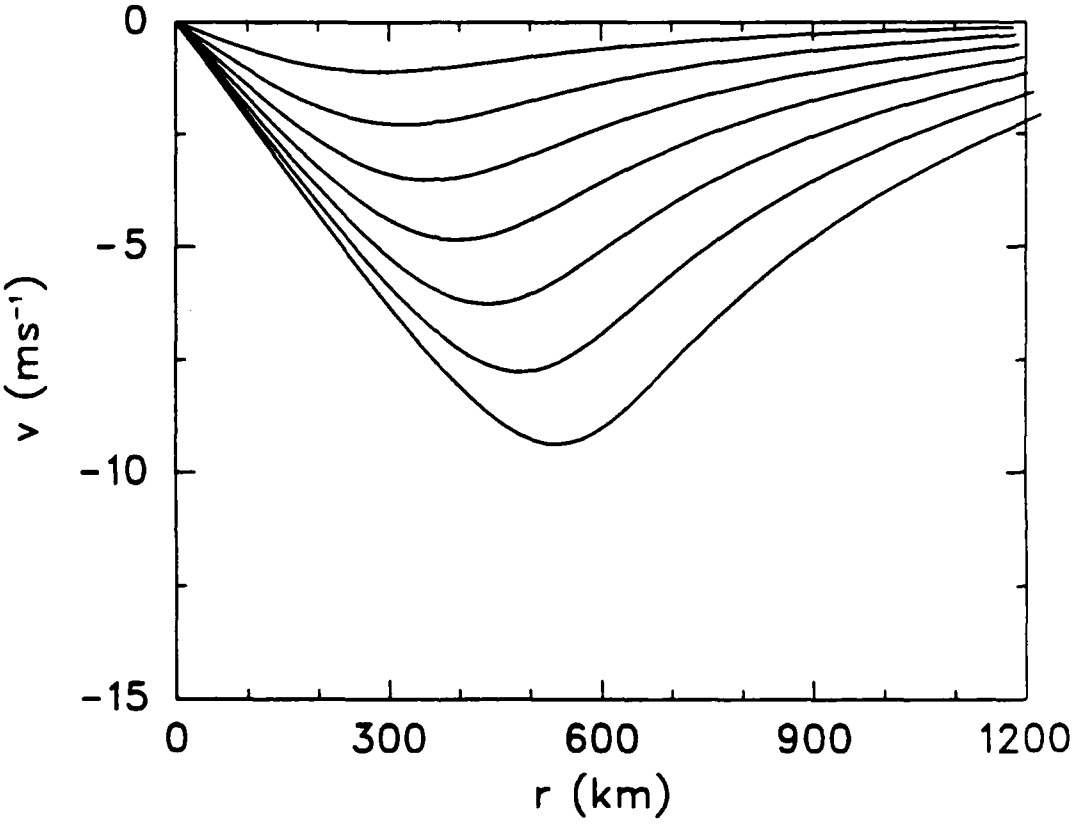

Figure 6.17: The tangential wind (v) as a function of r for layer two corresponding to $T = 1, 2, \ldots, 7$ days.

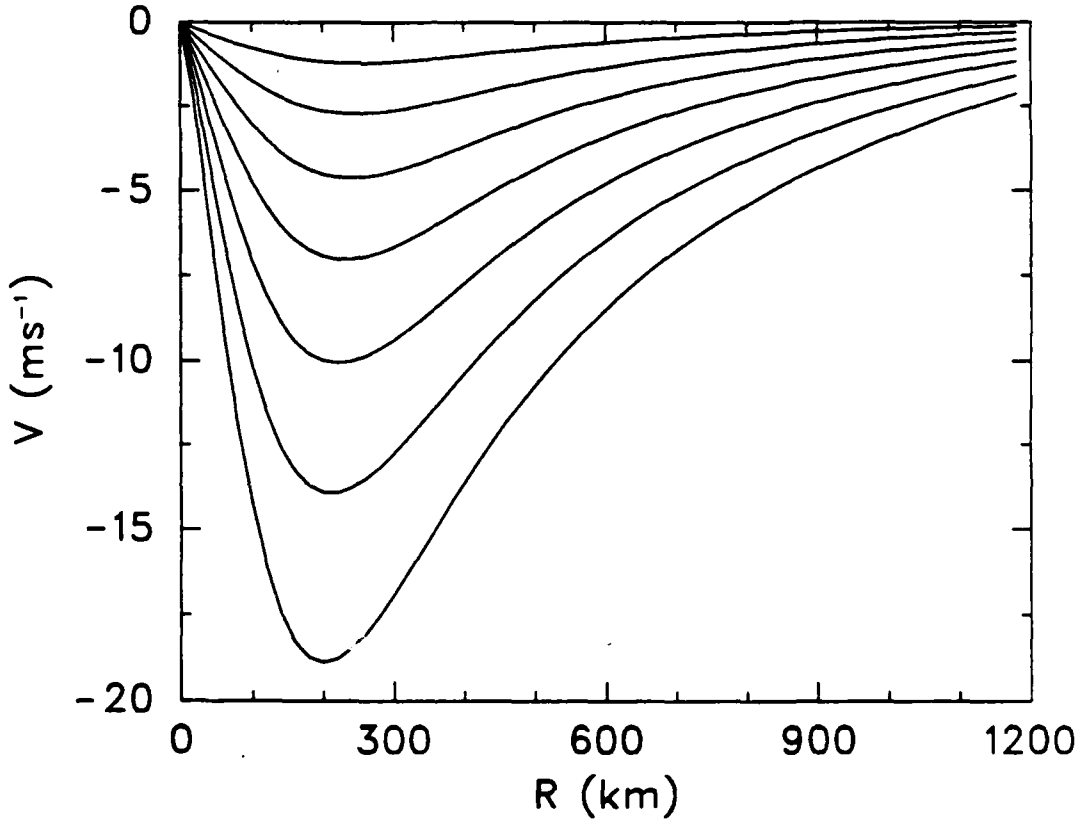

Figure 6.18: V as a function of R for layer two corresponding to $T = 1, 2, \ldots, 7$ days.

time at the center. However, due to the crude lateral boundary condition the outer region is somewhat anomalous. We get increasing, slightly cyclonic vorticity. This is caused by requiring the average vorticity be zero.

Chapter 7

SUMMARY AND CONCLUSIONS

We have attempted to solve the invertibility principle for Ooyama's tropical cyclone model using potential vorticity reasoning and potential radius coordinates. Presentation of potential vorticity and potential radius in a shallow water model showed how they are used to an advantage. They provide stretching in regions of large vorticity for better resolution and eliminate the radial component of the wind from the problem.

We showed that the invertibility principle can be written and solved several different ways. Solving for Φ or h using the shooting method works very well. However, these methods can not be generalized to two layers, because the secant method only works for problems of a single variable. Solving for h using a nonlinear equation solver "black box" also worked well. Again this was difficult to transport to the full model, because we were not able to uniquely define the problem in this case. Solving a tridiagonal matrix equation for V looked promising, but proved disappointing. This method produced only a weak vortex, because the matrix solver was too sensitive to small changes in the vorticity. Finally, solving for V with the nonlinear equation solver proved the best. Although somewhat slow, this produced good results and generalized easily to two layers.

We next looked at Ooyama's model and how it solved for the wind field. This model is based on gradient balanced, axisymmetric flow in a homogeneous incompressible fluid. Prediction is based on the radial mass flux and involves solving a system of three coupled pairs of equations. The results show a vortex which evolves into a tropical cyclone after approximately six days. The structure and evolution are in strong agreement with observational data.

Our tropical cyclone model incorporates the potential radius ideas as in the shallow water case. Although we include friction in this case, the advantages of coordinate stretching and elimination of the radial wind component remain. The invertibility is derived and solved using the nonlinear equation solver. It is interesting to note that the problem has been reduced to one coupled pair of equations.

Through this analysis we have shown a different way of looking at tropical cyclones. The release of latent heat produces positive relative vorticity at low levels and negative relative vorticity at upper levels. This in turn produces cyclonic winds at low levels and anticyclonic winds at upper levels. The wind and mass fields mutually adjust to the production of potential vorticity anomalies by latent heat release.

This work has shown that it is possible to create a tropical cyclone model using potential vorticity as the predictive variable. However, more work needs to be done to close the system and make it a true tropical cyclone model. The boundary layer must be added to include the air-sea interchange of moisture and surface frictional effects. A parameterization of cumulus convection needs to be added to more accurately describe the release of latent heat. It would also be useful to make the model less restrictive by allowing the user to specify the initial wind field, the sea surface temperature, and the latitude. This way the model could be used to examine different initial conditions in different locations.

REFERENCES

Burden, R. L. and J. D. Faires, 1985: *Numerical Analysis*, third edition. Boston, Prindle, Weber & Schmidt, Chaps 2, 5, 6, and 10.

Eliassen, A., 1952: Slow thermally or frictionally controlled meridional circulation in a circular vortex. *Astrophys. Norv.*, **5**, 19–60.

Ertel, H., 1942: Ein neuer hydrodynamischer wirbelsatz. *Met. Z.*, **59**, 271–281.

Hack, J. J., and W. H. Schubert, 1986: Nonlinear response of atmospheric vortices to heating by organized cumulus convection. *J. Atmos. Sci.*, **43**, 1559–1573.

Haltiner, G. J., and R. T. Williams, 1980: *Numerical Prediction and Dynamic Meteorology*, second edition. New York, John Wiley & Sons, 83.

Haynes, P. H., and M. E. McIntyre, 1987: On the evolution of vorticity and potential vorticity in the presence of diabatic heating and frictional or other forces. *J. Atmos. Sci.*, **44**, 828–841.

Holton, J. R., 1979: *An Introduction to Dynamic Meteorology*, second edition. New York, Academic Press, 242–244.

Hoskins, B. J. and F. P. Bretherton, 1972: Atmospheric frontogenesis models: mathematical formulation and solution. *J. Atmos. Sci.*, **29**, 11–37.

Hoskins, B. J., M. E. McIntyre and A. W. Robertson, 1985: On the use and significance of isentropic potential vorticity maps. *Quart. J. R. Met. Soc.*, **111**, 877–946.

Kahaner, D., C. Moler, and S. Nash, 1989: *Numerical Methods and Software*. Englewood Cliffs, NJ, Prentice Hall, 258–260.

Kleinschmidt, E., 1950a: Über aufbau und entstehung von zyklonen (1. Teil). *Met. Runds.*, **3**, 1–6.

—, 1950b: Über aufbau und entstehung von zyklonen (2. Teil). *Met. Runds.*, **3**, 54–61.

—, 1951: Über aufbau und entstehung von zyklonen (3. Teil). *Met. Runds.*, **4**, 89–96.

—, 1955: Die entstehung einer höhenzyklone über nordamerika, *Tellus*, *7*, 96–110.

—, 1957: In 'Dynamic meteorology' by Eliassen, A. and Kleinschmidt, E., *Handbuch der physik*, **48**, 112–129.

Ooyama, K., 1969: Numerical simulation of the life cycle of tropical cyclones. *J. Atmos. Sci.*, **26**, 2–40.

Rossby, C. G., 1939: Relation between variations in the intensity of the zonal circulation of the atmosphere and the displacements of the semi-permanent centers of action. *J. Marine Res.*, **2**(1), 38–55.

—, 1940: Planetary flow patterns in the atmosphere. *Quart. J. R. Met. Soc.*, **66**, Suppl., 68–87.

Schubert, W. H., and B. T. Alworth, 1987: Evolution of potential vorticity in tropical cyclones. *Quart. J. R. Met. Soc.*, **113**, 147–162.

Schubert, W. H., and M. DeMaria, 1985: Axisymmetric, Primitive Equation, Spectral Tropical Cyclone Model. Part I: Formulation. *J. Atmos. Sci.*, **42**, 1213–1224.

Schubert, W. H., and J. J. Hack, 1983: Transformed Eliassen balanced vortex model. *J. Atmos. Sci.*, **40**, 1571–1583.

Schubert, W. H., E. Ruprecht, P. E. Ciesielski, and H. Kuo, 1986: Ertel's potential vorticity: English translations of Ertel's original papers on potential vorticity conservation principles. Available from first author, Colorado State University, Fort Collins.

Shutts, G. J., M. Booth, and J. Norbury, 1988: A Geometric Model of Balanced, Axisymmetric Flows with Embedded Penetrative Convection. *J. Atmos. Sci.*, **45**, 2609–2621.

Shutts, G. J., and A. J. Thorpe, 1978: Some aspects of vortices in rotating, stratified fluids. *Pure Appl. Geophys.*, **116**, 993–1006.